

การเกิดเคออนและซิกมาเมซอนในการชนของไอออนหนักที่ระดับ

พลังงานปานกลาง

นางสาวพรรณรัตน์ ศรีสวัสดิ์

วิทยานิพนธ์นี้เป็นส่วนหนึ่งของการศึกษาตามหลักสูตรปริญญาวิทยาศาสตรดุษฎีบัณฑิต

สาขาวิชาฟิสิกส์

มหาวิทยาลัยเทคโนโลยีสุรนารี

ปีการศึกษา 2549

ISBN 974-533-595-9

**KAON AND SIGMA MESON PRODUCTION  
IN HEAVY ION COLLISIONS AT  
INTERMEDIATE ENERGIES**

**Pornrad Srisawad**

**A Thesis Submitted in Partial Fulfillment of the Requirements  
for the Degree of Doctor of Philosophy in Physics**

**Suranaree University of Technology**

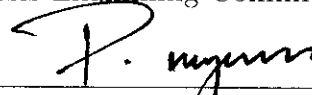
**Academic Year 2006**

**ISBN 974-533-595-9**

**KAON AND SIGMA MESON PRODUCTION  
IN HEAVY ION COLLISIONS  
AT INTERMEDIATE ENERGIES**

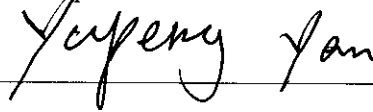
Suranaree University of Technology has approved this thesis submitted in partial fulfillment of the requirements for the Degree of Doctor of Philosophy.

Thesis Examining Committee



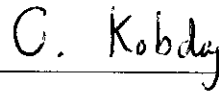
(Assoc. Prof. Dr. Prapun Manyum)

Chairperson



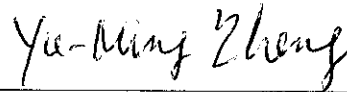
(Assoc. Prof. Dr. Yupeng Yan)

Member (Thesis Advisor)



(Asst. Prof. Dr. Chinorat Kobdaj)

Member



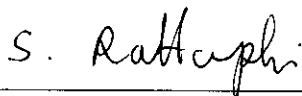
(Prof. Yu-Ming Zheng)

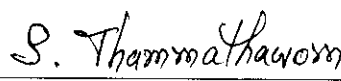
Member



(Assoc. Prof. Dr. Prasart Suebka)

Member





(Assoc. Prof. Dr. Saowanee Rattanaphani) (Assoc. Prof. Dr. Sompong Thammathaworn)

Vice Rector for Academic Affairs

Dean of Institute of Science

พริตต์ ศรีสวัสดิ์ : การเกิดเคออนและซิกมาเมซอนในการชนของไอออนหนักที่ระดับพลังงานปานกลาง (KAON AND SIGMA PRODUCTION IN HEAVY ION COLLISIONS AT INTERMEDIATE ENERGIES) อาจารย์ที่ปรึกษา : รองศาสตราจารย์ ดร. ยูเป็ง แยน, 76 หน้า. ISBN 974-533-595-9

วิทยานิพนธ์นี้ศึกษาเชิงทฤษฎีเกี่ยวกับการเกิดเคออนและซิกมาเมซอนในการชนของไอออนหนักที่ระดับพลังงานปานกลาง การวิวัฒนาการของนิวเคลียสที่เข้าชนกันสามารถอธิบายได้ภายใต้กรอบของพลศาสตร์ควอนตัมเชิงโมเลกุล (QMD)

เราพิจารณาพลังงานของการชนในช่วง 0.85 ถึง 2 จิกะอิเล็กตรอน โวลต์ต่อนิวเคลียส สำหรับการเกิดเคออนที่มีประจุบวก โดยเคออนที่มีประจุบวกถูกคาดหมายว่าเป็นเครื่องมือที่ดีที่สุดที่ใช้ในการตรวจสอบสัณฐานของเคออนในตัวกลางและสมการสถานะทางนิวเคลียร์ (EOS) ในการศึกษาครั้งนี้ เราวิเคราะห์การไหลเชิงระนาบของเคออนที่มีประจุบวกและวิเคราะห์การกระจายของพลังงานจลน์ของภาคตัดขวางในการเกิดเคออนที่มีประจุบวก ซึ่งพบว่าแรงลอเรนตซ์จากองค์ประกอบทางตำแหน่งของสนามเวกเตอร์มีความสำคัญต่อพลวัตของเคออนในตัวกลางและยังสามารถหักล้างกับผลของสัณฐานเวกเตอร์ในการไหลของเคออนที่มีประจุบวกในแนวระนาบ ข้อมูลจาก FIPO สามารถอธิบายได้โดยใช้สัณฐานของเคออนในตัวกลางบนพื้นฐานของแบบจำลองเชิงไคแรลยังผล ข้อมูลของสัณฐานเคออนที่มีประจุบวกในตัวกลางที่ถูกนำมาจากการไหลของเคออนและภาคตัดขวางในการเกิดเคออนที่มีประจุบวกนี้เป็นฟังก์ชันของพลังงานจลน์ที่จุดศูนย์กลางมวลซึ่งมีความสอดคล้องกับข้อมูลจากแหล่งอื่น ข้อมูลที่ได้จากการศึกษาในวิทยานิพนธ์นี้ยืนยันว่าการใช้สมการสถานะทางนิวเคลียร์แบบอ่อนสามารถอธิบายภาคตัดขวางของการเกิดเคออนที่มีประจุบวกได้ดีกว่า

ซิกมาเมซอนเป็นอนุภาคเรโซแนนซ์ที่ไม่เสถียรและส่วนใหญ่จะสลายตัวไปเป็นไพออน 2 อนุภาคในปริภูมิอิสระ การศึกษาในเชิงทฤษฎีในระยะหลังนี้พบว่า มวล ( $m_\sigma$ ) และความกว้าง ( $\Gamma_\sigma$ ) ซิกมาเมซอนมีค่าลดลงอย่างมากเมื่อนิวเคลียสมีความหนาแน่นเพิ่มขึ้น ซึ่งหมายความว่าซิกมาเมซอนอาจคงอยู่ได้ในสถานะของนิวเคลียสที่มีความหนาแน่นสูง ปรากฏการณ์นี้เป็นสิ่งที่น่าสนใจอย่างยิ่งในการค้นคว้าเพิ่มเติมถึงการเปลี่ยนแปลงคุณสมบัติของซิกมาเมซอนในตัวกลางที่ได้จากนิวเคลียส ในวิทยานิพนธ์นี้เราได้ศึกษาการเกิดซิกมาเมซอนที่ได้จากการชนของโปรตอนพลังงาน 0.85 และ 1.5 จิกะอิเล็กตรอน โวลต์ต่อนิวเคลียสของคาร์บอน 12 แคลเซียม 40 และตะกั่ว 208 ผลการศึกษาโดยใช้การจำลองทางคอมพิวเตอร์ระบุว่า การเกิดซิกมาเมซอนจะขึ้นกับเลขมวลอย่างเห็นได้ชัด โดยเมื่อเลขมวลมีค่าเพิ่มขึ้นจะส่งผลให้ค่าภาคตัดขวางของการเกิดซิกมาเมซอนมีค่าเพิ่มขึ้นตามไปด้วย นอกจากนี้ยังพบอีกว่าการเกิดซิกมาเมซอนในปฏิกิริยาที่มีการเหนี่ยวนำโปรตอนจะ

ชนิดของตัวกลางอย่างมาก และการเกิดการสลายตัวของซิกมาเมซอนในตัวกลางที่มีความหนาแน่นสูงกว่าจะมีการเปลี่ยนแปลงไปในทางที่ทำให้มวลลดลง การเปลี่ยนมวลนี้สามารถสังเกตได้ในการทดลองซึ่งสถานะสุดท้ายของคู่อิพออน ไม่ถูกดูดกลืนโดยนิวคลีออนแวดล้อม จากการศึกษาข้างชี้ให้เห็นอีกว่าอัตราส่วนของภาคตัดขวางซิกมาเมซอนที่เป็นฟังก์ชันของมวลขึ้นยงจากปฏิกิริยาต่าง ๆ เปิดโอกาสให้ทำการทดลองการเปลี่ยนของมวลของซิกมาเมซอนในสภาวะแวดล้อมนิวเคลียสที่มีความหนาแน่นสูงได้

สาขาวิชาฟิสิกส์  
ปีการศึกษา 2549

ลายมือชื่อนักศึกษา ชวรัตน์ ๗๖๖๖๖๖  
ลายมือชื่ออาจารย์ที่ปรึกษา Jupeng Yan  
ลายมือชื่ออาจารย์ที่ปรึกษาร่วม ชวรัตน์ ๗๐๗๑๔  
ลายมือชื่ออาจารย์ที่ปรึกษาร่วม Yu-Hing Zhang

PORNRAD SRISAWAD : KAON AND SIGMA MESON PRODUCTION  
IN HEAVY ION COLLISIONS AT INTERMEDIATE ENERGIES.

THESIS ADVISOR : ASSOC. PROF. YUPENG YAN, Ph.D. 76 PP.

ISBN 974-533-595-9

HEAVY ION REACTION/KAON AND SIGMA MESON/THE CHIRAL SYM-  
METRY/THE QUANTUM CHROMODYNAMICS (QCD)/THE QUANTUM  
MOLECULAR DYNAMICS(QMD)/THE  $K^+$  IN-PLANE FLOW/ THE IN-  
MEDIUM KAON POTENTIAL/THE NUCLEAR EQUATION OF STATE/THE  
PRODUCTION CROSS SECTIONS

This thesis is devoted to the theoretical study of the kaon and sigma meson productions in heavy ion reactions at intermediate energies. The time evolution of the colliding nuclei is described within the framework of the Quantum Molecular Dynamics (QMD).

We considered the bombarding energies in the 0.8-2 GeV per nucleon for  $K^+$  production. It is thus expected that the  $K^+$  is a very ideal tool to probe the in-medium kaon potential and the nuclear equation of state (EOS). In the present study we have analyzed the  $K^+$  in-plane flow and the kinetic energy distributions of  $K^+$  production cross sections. It is found that the Lorentz force from spatial component of the vector field provides an important contribution to the in-medium kaon dynamics and strongly counterbalances the influence of the vector potential on the  $K^+$  in-plane flow. The FOPI data can reasonably be described using the in-medium kaon potential based on effective chiral models. The information on the in-medium  $K^+$  potential extracted from the kaon flow and the  $K^+$  production

cross section as a function of their center-of-mass kinetic energy is consistent with the knowledge from other sources. It is confirmed that data of the  $K^+$  production cross sections are better described when a soft EOS is used.

The  $\sigma$  meson is a broad scalar resonance and mainly decays into two pions in free space. Recently, theoretical studies have shown that the  $\sigma$  mass ( $m_\sigma$ ) and width ( $\Gamma_\sigma$ ) dramatically decrease with increasing of the nuclear density ( $\rho$ ), which means that the sigma meson may exist in a dense nuclear environment. This causes great interest to further explore the modification of sigma meson properties in nuclear medium. We investigate the sigma meson productions in 0.85 and 1.5 GeV proton colliding on nuclei of  $^{12}\text{C}$ ,  $^{40}\text{Ca}$ , and  $^{208}\text{Pb}$ . The simulation results indicate a distinctive  $A$  dependence of the sigma meson production, in which the increase of  $A$  is followed by that of the production cross sections. It is found that the  $\sigma$  meson production in proton induced reactions is strongly medium-dependent, and the produce  $\sigma$  meson decaying in a denser medium experiences a stronger mass shift towards lower masses. This mass shift is an experimentally accessible observation in the final state pion pairs which does not suffer reabsorption by the surrounding nucleons. It is pointed out that the ratio of measured sigma meson cross section as a function of the sigma meson invariant-mass from various reactions opens the possibility to experimentally address the mass shift of the  $\sigma$  meson in a dense nucleus environment.

School of Physics

Academic Year 2006

Student's Signature Pornrod Srisanood

Advisor's Signature Yupeng Yan

Co-advisor's Signature C. Kobdaj

Co-advisor's Signature Yu-King Zhang

## ACKNOWLEDGEMENTS

I am grateful to Assoc. Prof. Dr. Yupeng Yan and Asst. Prof. Dr. Chinorat Kobdaj for being my thesis advisor and co-advisor. They set up the research project cooperations with Prof. Yu-Ming Zheng from China Institute of Atomic Energy of China and Prof. Amand Faessler in Tuebingen, Germany that give me a very good research experience and was the starting point of this work.

I would like to thank Prof. Yu-Ming Zheng and Prof. Dr. Christian Fuchs for their guidance, consistently helpful advices throughout this work and their kind hospitality during my research started at Institute for Theoretical Physics, University of Tuebingen, Germany over one year.

I would like to thank Assoc. Prof. Dr. Prasart Suebka and Assoc. Prof. Dr. Prapun Manyum for their kindness and being Thesis Examining Committee.

I wish to thank Mr. Thomas Bauer, Mr. Ayut Limphirat, Mr. Suppiya Siranan, Dr. Khanchai Khosonthongkee, Dr. Nattapong Yongram, Dr. Kem Pumsa-ard and Dr. Jessada Tanthanuch for their consistent helps, especially in building up thesis format.

I acknowledge the financial supports by Ministry of Education, Thailand, Naresuan University, the National Research Council of Thailand (NRCT) under Grant No. 1.CH5/2549, by the Deutsche Forschungsgemeinschaft (DFG) under Grant No. 446CHV-113/91/1-3 and by the National Natural Science Foundation of China (NSFC) under Grant Nos. 10435080, 10575075 and 10447006.

Finally, I would like to thank my parents and my sister for their understanding, support and encouragement over the years of my study.

Pornrad Srisawad



# CONTENTS

	Page
ABSTRACT IN THAI . . . . .	I
ABSTRACT IN ENGLISH . . . . .	III
ACKNOWLEDGEMENTS . . . . .	V
CONTENTS . . . . .	VI
LIST OF TABLES . . . . .	VIII
LIST OF FIGURES . . . . .	IX
 <b>CHAPTER</b>	
<b>I INTRODUCTION . . . . .</b>	<b>1</b>
<b>II BRIEF DESCRIPTION OF THE QUANTUM MOLECULAR DYNAMICS . . . . .</b>	<b>5</b>
2.1 Initialization . . . . .	6
2.2 Propagation . . . . .	9
2.3 Collision . . . . .	14
<b>III KAON MESON PRODUCTION IN HEAVY ION COLLISIONS . . . . .</b>	<b>22</b>
3.1 Kaon covariant dynamics . . . . .	22
3.2 Kaon production in the QMD model . . . . .	25
3.3 Results and discussions . . . . .	28
<b>IV SIGMA MESON PRODUCTION IN HEAVY ION COLLISIONS . . . . .</b>	<b>42</b>
4.1 Sigma meson production in elementary reactions . . . . .	42
4.2 $\pi\pi$ interaction . . . . .	44

## CONTENTS (Continued)

	<b>Page</b>
4.2.1 $\pi\pi$ interaction in Vacuum . . . . .	45
4.2.2 $\pi\pi$ interaction in nuclear medium. . . . .	46
4.3 Sigma meson production in the QMD model . . . . .	49
4.4 Results and discussions . . . . .	50
<b>V SUMMARY . . . . .</b>	<b>61</b>
REFERENCES . . . . .	65
CURRICULUM VITAE . . . . .	76

# LIST OF TABLES

Table		Page
2.1	The parameters of Eq. (2.20) for the hard (H) and the soft (S) EOS.	14
2.2	List of $N^*$ resonances which are included in the QMD model. The table shows the resonance masses and the total and partial widths of the included decay channels in MeV. For details, please see the work (Shekgter, Christian, Amand Faessler and Krivoruchenko, 2003).	16
2.3	List of $\Delta$ resonances which are included in the QMD model. The table shows the resonance masses, and the total and partial widths of the included decay channels in MeV. For details, please see the work (Shekgter, Christian, Amand Faessler and Krivoruchenko, 2003).	17

# LIST OF FIGURES

Figure	Page
2.1	Equation of state. The density dependence of the energy per particle in nuclear matter at temperature $T = 0$ is displayed for two different sets of parameters . . . . . 13
2.2	Inclusive $\pi^-p$ and $\pi^+p$ cross sections obtained by the sum over all resonances which are taken into account in the present description . 21
3.1	Diagrammatic representation of the reaction $BB \rightarrow BYK^+$ . . . . 27
3.2	The $K^+$ transverse flow as a function of rapidity in 1.93 A GeV Ni + Ni reactions (Zheng, Fuchs, Amand Faessler, Shekhter, Srisawad, Kobdaj and Yan, 2004). . . . . 29
3.3	The $K^+$ excitation functions in Au + Au (scaled by $10^{-1}$ ) and C + C reactions are compared to the KaoS data. Calculations include an in-medium kaon potential. For C + C results without in-medium kaon potential are also shown (Fuchs, Amand Faessler Zabrodin and Yu-Ming Zheng, 2001). . . . . 31
3.4	Inclusive $K^+$ production cross section for Ni + Ni collisions at 0.8 GeV/nucleon as a function of the c.m. kinetic energy. Calculations are performed using a soft nuclear EOS with and without kaon potential. . . . . 33
3.5	Inclusive $K^+$ production cross section for Ni + Ni collisions at 1 GeV/nucleon as a function of the c.m. kinetic energy. Calculations are performed using a soft nuclear EOS with and without kaon potential. . . . . 34

## LIST OF FIGURES (Continued)

Figure		Page
3.6	Inclusive $K^+$ production cross section for Ni + Ni collisions at 1.8 GeV/nucleon as a function of the c.m. kinetic energy. Calculations are performed using a soft nuclear EOS with and without kaon potential. . . . .	35
3.7	Inclusive $K^+$ production cross section for Ni + Ni collisions at 0.8 GeV/nucleon as a function of the c.m. kinetic energy. Calculations are performed using a hard nuclear EOS with and without kaon potential. . . . .	36
3.8	Inclusive $K^+$ production cross section for Ni + Ni collisions at 1 GeV/nucleon as a function of the c.m. kinetic energy. Calculations are performed using a hard nuclear EOS with and without kaon potential. . . . .	37
3.9	Inclusive $K^+$ production cross section for Ni + Ni collisions at 1.8 GeV/nucleon as a function of the c.m. kinetic energy. Calculations are performed using a hard nuclear EOS with and without kaon potential. . . . .	38
3.10	Inclusive $K^+$ production cross sections for Ni + Ni collisions at 0.8 GeV/nucleon as a function of the c.m. kinetic energy. Calculations are performed with an in-medium kaon potential and a hard/soft nuclear EOS. . . . .	39

## LIST OF FIGURES (Continued)

Figure	Page	
3.11	Inclusive $K^+$ production cross sections for Ni + Ni collisions at 1 GeV/nucleon as a function of the c.m. kinetic energy. Calculations are performed with an in-medium kaon potential and a hard/soft nuclear EOS. . . . .	40
3.12	Inclusive $K^+$ production cross sections for Ni + Ni collisions at 1.8 GeV/nucleon as a function of the c.m. kinetic energy. Calculations are performed with an in-medium kaon potential and a hard/soft nuclear EOS. . . . .	41
4.1	diagrammatic representation of the BS equation for $\pi\pi$ scattering in vacuum. . . . .	46
4.2	Terms of the meson-meson scattering amplitude accounting for $ph$ and $\Delta h$ excitations . . . . .	47
4.3	$\sigma$ mass and half width as the functions of the nuclear density. Dashed lines include also the $2ph$ pion selfenergy pieces. . . . .	48
4.4	The distribution of the $\pi$ number produced in the p + A reactions with A being $^{12}C$ , $^{40}Ca$ and $^{208}Pb$ at the incident energy 1.5 GeV at the impact parameter $b = 0$ . . . . .	51
4.5	The $\sigma$ meson creation and decay as the function of the nuclear density ( $\rho$ ) in the p + A reactions with A being $^{12}C$ , $^{40}Ca$ and $^{208}Pb$ at the incident energy 1.5 GeV at the impact parameter $b = 0$ . . .	53
4.6	The $\sigma$ creation and decay probabilities as the function of time (fm/c) in the p + A reactions with A being $^{12}C$ , $^{40}Ca$ and $^{208}Pb$ at the incident energy 1.5 GeV at the impact parameter $b = 0$ . . .	55

## LIST OF FIGURES (Continued)

Figure		Page
4.7	<p>The invariant-mass distribution of the sigma mesons produced in the <math>p + A</math> reactions with <math>A</math> being <math>^{12}C</math>, <math>^{40}Ca</math> and <math>^{208}Pb</math> at the incident energies 0.85 GeV and 1.5 GeV. Solid lines: produced <math>\sigma</math> without medium modifications of the <math>\sigma</math> meson. Dashed lines: measured <math>\sigma</math> without medium modifications of the <math>\sigma</math> meson. Dot Dashed lines: produced <math>\sigma</math> with medium modifications of the <math>\sigma</math> meson. Dot lines: measured <math>\sigma</math> with medium modifications of the <math>\sigma</math> meson. . . .</p>	57
4.8	<p>Ratio of the sigma cross sections in various collisions. Solid lines: produced <math>\sigma</math> without medium modifications of the <math>\sigma</math> meson. Dashed lines: measured <math>\sigma</math> without medium modifications of the <math>\sigma</math> meson. Dot Dashed lines: produced <math>\sigma</math> with medium modifications of the <math>\sigma</math> meson. Dot lines: measured <math>\sigma</math> with medium modifications of the <math>\sigma</math> meson. . . . .</p>	59

# CHAPTER I

## INTRODUCTION

In this thesis the kaon and sigma meson productions in heavy ion reactions at intermediate energies are investigated within the framework of the Quantum Molecular Dynamics (QMD). One of the main motivations of the study is to obtain the information of the modifications of hadron properties in dense and hot matters and to explore the properties of nuclear matters at high densities, i.e. the nuclear equation of state (EOS) at supra-normal densities. This issue is very important not only for nuclear and particle physics, but also for astrophysics.

Hadrons are expected to change their masses in a nuclear matter compared to free space. It is known from the Quantum Chromodynamics (QCD) that the spontaneous chiral symmetry breaking is signalled by non-vanishing quark pair condensates in vacuum (Weise, 1993). According to the Gell-Mann, Oakes, Renner (GOR) relation (Gell-Mann, Oakes and Renner, 1968). the vacuum condensates enter the expression of pion mass:

$$m_\pi^2 f_\pi^2 = -\frac{1}{2}(m_u - m_d)\langle uu + dd \rangle, \quad (1.1)$$

where  $m_u$  and  $m_d$  are respectively the bare masses of the  $u$  and  $d$  quarks and the pion decay constant  $f_\pi = 93.3$  MeV. For kaons the corresponding relation reads

$$m_K^2 f_K^2 = -\frac{1}{2}(m_u - m_s)\langle uu + ss \rangle, \quad (1.2)$$

where  $m_s$  is the bare mass of the strange quark. The strange quark condensate  $\langle ss \rangle$  is of the same order of magnitude as the  $\langle uu \rangle \simeq \langle dd \rangle \simeq -(230 \pm 25 \text{ MeV})^3$  (Kogut, Sinclair and Wang, 1991). However, an increasing density or temperature tends



to wash out the quark condensates, and thus partially restore chiral symmetry. Adding nucleons to the vacuum implies a change of the average scalar density. To leading order in density ( $\rho$ ), one obtains the change of the quark condensates with density

$$\frac{\langle qq \rangle_\rho}{\langle \bar{q}q \rangle_{\rho=0}} = 1 - \frac{\Sigma_{\pi N}}{m_\pi^2 f_\pi^2} \rho + \dots, \quad (1.3)$$

with the pion-nucleon Sigma term (Gasser, Leutwyler and Sainio, 1991)

$$\Sigma_{\pi N} = (m_u + m_d) \langle N | \bar{q}q | N \rangle = (45 \pm 8) \text{ MeV}, \quad (1.4)$$

where  $\langle N | \bar{q}q | N \rangle$  is the nucleon matrix element of the scalar quark density. Similarly, one gets the variation of the quark condensates with the temperature (Gasser and Leutwyler, 1987; Gerber and Leutwyler, 1989).

$$\frac{\langle \bar{q}q \rangle_T}{\langle \bar{q}q \rangle_{T=0}} = 1 - \frac{N_f^2 - 1}{3T_f} \left( \frac{T}{2f_\pi} \right)^2 + \dots \quad (1.5)$$

Here  $N_f$  is Flavor number. It is seen from the above two equations that the quark condensates decrease with increasing the density and temperature, indicating a strong tendency towards chiral symmetry restoration. The change of the condensates by a nuclear environment will give rise to an average scalar potential experienced by the hadron in the medium, which shifts the hadron mass from its value in free space.

The hadron mass variation could have significant consequence if the surrounding nuclear matter is extremely dense and hot. For instance, a strong mass reduction for antikaons may favor  $K^-$  condensation at high nuclear densities and thus modified the mass of neutron stars to the values of about 1.5 times the solar mass, which is close to astronomic observations (Bethe and Brown, 1995; Li, Lee and Brown, 1997). It is noticed that the pion condensation is unlikely to appear due to the Goldstone Boson nature of the pions (Dickhoff et al., 1981; Lutz, Klimt and Weise, 1992). The idea is that, not only the quark condensates, but the pion

decay constant is also subject to medium modifications according to the Brown-Rho scaling, i.e.  $\frac{f_\pi(\rho)}{f_\pi(\rho=0)} = \left(\frac{\langle\bar{q}q\rangle_\rho}{\langle\bar{q}q\rangle_{\rho=0}}\right)^{1/2}$  (Brown and Rho, 1991). Thus the GOR relation for pions remains satisfied even in the medium. As a consequence, any significant variation of the pion mass in the medium is impossible.

It is known that the  $\sigma$  meson is responsible for the medium-range nucleon-nucleon attraction (Machleidt, Holinde and Elster, 1986). and plays an important role in the Quantum Hadrodynamics (QHD) (Walecka, 1974; Boguta and Bodmer, 1977). and the nonlinear sigma model (Petropoulos, 2004). However, the  $\sigma$  meson is a broad scalar resonance, i.e. its mass  $m_\sigma = 400 - 1200$  MeV and its width  $\Gamma_\sigma = 600 - 1000$  MeV, indicating that it is a short-lived resonance with a lifetime  $\tau \approx 10^{-24}$  second, which is the time scale of strong interactions. The large width of the sigma meson prevents a direct measurement of its invariant mass distribution over a non-resonant background. Thus the  $\sigma$  meson is commonly treated as an effective meson, that is, as a system of two pions coupled to the  $I = J = 0$  channel but not necessarily bound.

Recently theoretical studies show that the  $\sigma$  mass ( $m_\sigma$ ) and width ( $\Gamma_\sigma$ ) decrease dramatically with increasing of the nuclear density ( $\rho$ ) (Vicente Vacas and Oset, 2002). This means that the sigma meson may exist in a dense nuclear environment. There are also number of experimental efforts to evidence the existence of the sigma meson by pion (Bonutti et al., 1999; Camerini, Grion and Rui, 1993; Starostin et al., 2000). and photon (Messchendorp et al., 2002; Wolf et al., 2000). induced reactions on nuclei. This causes great interest to explore further the modification of sigma meson properties in nuclear medium.

The reduction of hadron masses in the medium results in a mean field experienced by the hadrons. Such an in-medium mean field will certainly manifest itself in heavy ion collisions and modify final state properties of the hadrons. So,

one can extract the information on the in-medium potentials of hadrons from the analysis of observables, which are sensitive to the change of final state properties of these hadrons.

Heavy ion collisions at intermediate energies about 0.8 - 2 A GeV provide the possibility to create the compressed nuclear matter with densities of about 2 to  $4\rho_0$ . Here  $\rho_0 \simeq 0.16 \text{ fm}^{-3}$  is the saturation density. This energy region is close to or below the  $K^+$  production threshold for free nucleon-nucleon collisions. Subthreshold kaon production is particularly interesting since it ensures that the kaon originates from the high density phase of the reaction. The missing energy has to be provided either by the Fermi motion of the nucleons or by energy accumulating multi-step reactions. Both processes exclude significant distortions from surface effects if one goes sufficiently far below threshold. It is known from the strangeness conservation that  $K^+$  mesons, once produced, can not be absorbed by the surrounding nucleons. This results in a rather long mean free path of about 7 fm of  $K^+$  mesons in nuclear matter and makes them a suitable 'penetrating' probe for the dense fireball produced in heavy ion reactions. Final state interactions such as elastic kaon-nucleon scattering or the propagation in potentials influence the dynamics but do not change the total yields. Therefore the Subthreshold  $K^+$  production is an ideal tool to probe the compressed nuclear matter, i.e. to explore the nuclear EOS at supra-normal densities, in relativistic heavy ion reactions (Aichelin and Che Ming Ko, 1985).

This thesis is organized as follows. Given in Chapter II is a brief description of the Quantum Molecular Dynamics. In Chapter III we study the kaon meson production in heavy ion collisions. Chapter IV is devoted to the study of the sigma meson production in heavy ion reactions. The final chapter of the thesis gives a summary of the results obtained.

# CHAPTER II

## BRIEF DESCRIPTION OF THE QUANTUM MOLECULAR DYNAMICS

The structure of the Quantum Molecular Dynamics (QMD) can be best discussed when we start out with the classical molecular dynamics approach (Bodmer and Panos, 1977; Molitoris, Hoffer, Kruse and Stoecker, 1984). It is known that the classical molecular dynamics is a N-body theory. All information about the system is contained in the solution of the N body Liouville equation. The Boltzmann-Uhlenbeck-Uehling (BUU) or the Vlasov-Uhlenbeck-Uehling (VUU) approaches are genuine N-body theories. One follows the positions and momenta of all N particles and thus calculates the time evolution of the N-body density matrix. The numerical procedure to solve these equations is to get results through averaging over many ensembles, i.e. mixing correlations and fluctuations among different ensembles and rendering them useless. The predictive power of the BUU or VUU approach is therefore limited to one body observables.

Important quantum features are included in the QMD approach: collisions among nucleons are Pauli blocked when the scattered nucleons would enter already occupied or partially occupied phase space regions. Furthermore, the scattering amplitude does not relate the scattering angle with the impact parameter in a unique way: The square of the scattering amplitude is identified as a probability distribution. The scattering angle as well as the blocking of collisions which brings nucleons in a partially occupied phase space region are treated statistically. This procedure destroys the time reversibility of the classical equation. However, the

model is still the solution of the N-body equation, not a reduction to the one body level, and also describes the time evolution of all correlations.

These microscopic models are chaotic in the sense that the two neighboring phase space points in the  $A_T + A_P$  dimensional phase space diverge exponentially as a function of time. In a quantum system we cannot determine the impact parameter more precisely than  $\Delta b > \hbar/\Delta P$ . Instead of varying the impact parameter over this region we initialize the nuclei differently by drawing different random numbers for the position and the momentum of the particles.

To simulate heavy ion collisions in the QMD model, one faces two critical points: the initialization of the projectile and target nuclei and the time evolution of the  $A_T + A_P$  system. We start with the first point.

## 2.1 Initialization

When comparing quantal the time-dependent Hartree-Fock (TDHF) and the classical (Vlasov) mean field systems one finds an almost identical time evolution of the nuclear density for beam energies larger than 25 MeV per nucleon. Although the differential equations for the time evolution of the classical and quantal system are almost identical, this is quite surprising because of the different initial states. The initial density of the former calculation is given by a Slater determinant whereas the Vlasov equation starts with point like particles randomly distributed in a sphere of the radius  $r=1.14A^{1/3}$  fm, corresponding to a normal nuclear matter density of 0.16 nucleons/fm<sup>3</sup>. From these results one has concluded that, at the energies considered, the detailed form of the wave function has only minor influence on the time evolution of the bulk properties of the system, especially on the single particle observables.

In the QMD model each nucleon is represented by a coherent state of the

form ( we set  $\hbar, c=1$ )

$$\psi(\mathbf{r}, \mathbf{p}_0, t) = \frac{\exp[i\mathbf{p}_0 \cdot (\mathbf{r} - \mathbf{r}_0)]}{(2\pi L)^{3/4}} e^{-(\mathbf{r}-\mathbf{r}_0)^2/4L}. \quad (2.1)$$

where  $\mathbf{r}_0$  is the time dependent center of the Gaussian wave packet in coordinate space. The width of a coherent state increases as a function of time if it propagates with the free Schrödinger equation. In the QMD model the width  $L$  is kept constant, which means that one does not allow the spreading of the wave function. Otherwise, the whole nucleus would spread in coordinate space as a function of time.  $L$  is set to be  $L=1.08 \text{ fm}^2$  corresponding to a root mean square radius of the nucleon of 1.8 fm. To keep the formulation as close as possible to the classical transport theory, one uses Wigner density instead of working with wave function.

The Wigner transformation of the coherent states is Gaussians in momentum and coordinate space. Thus, the Wigner density reads

$$\begin{aligned} f(\mathbf{r}, \mathbf{p}, t) &= \frac{1}{(2\pi)^3} \int e^{-\mathbf{p} \cdot \mathbf{r}_{12}} \psi\left(\frac{\mathbf{r} + \mathbf{r}_{12}}{2}, t\right) \psi^*\left(\frac{\mathbf{r} - \mathbf{r}_{12}}{2}, t\right) d^3 \mathbf{r}_{12} \\ &= \frac{1}{(\pi)^3} \exp[-(\mathbf{r} - \mathbf{r}_0)^2/2L - (\mathbf{p} - \mathbf{p}_0)^2 \cdot 2L]. \end{aligned} \quad (2.2)$$

The  $N$  body Wigner density is the direct product of the Wigner densities of  $N$  coherent states

$$f^N(\mathbf{r}_1, \dots, \mathbf{r}_N; \mathbf{p}_1, \dots, \mathbf{p}_N; t) = \prod_{i=1}^N \frac{1}{(\pi)^3} e^{-(\mathbf{r}_i - \mathbf{r}_{i0})^2/2L - (\mathbf{p}_i - \mathbf{p}_{i0})^2 \cdot 2L}. \quad (2.3)$$

The wigner representation of our Gaussian wave packets obeys the uncertainty relation  $\Delta r_x \Delta p_x = \hbar/2$ . The density in coordinate space is given by the momentum integral over the Wigner density,

$$\begin{aligned} \rho(\mathbf{r}, t) &= \sum_{i=1}^N \delta(\mathbf{r} - \mathbf{r}_i) \int f^N(\mathbf{r}_1, \dots, \mathbf{r}_N; \mathbf{p}_1, \dots, \mathbf{p}_N; t) d^3 \mathbf{p}_1 \dots d^3 \mathbf{p}_N d^3 \mathbf{r}_1 \dots d^3 \mathbf{r}_N \\ &= \sum_i^N \frac{1}{(2\pi L)^{3/2}} e^{-(\mathbf{r} - \mathbf{r}_{i0})^2/2L}. \end{aligned} \quad (2.4)$$

A random choice of the centers of the  $A_T + A_P$  Gaussians in coordinate and momentum space is not sufficient to maintain the stability of the nuclei for a sufficiently long time . Due to fluctuations, a limited sequence of random numbers does not create the ground state of a nucleus but rather a metastable excited state which decays by emission of nucleons. The time span for which the nucleus is stable implies an upper limit to the excitation energy which can be tolerated.

Eigenstates of a Hamiltonian have to fulfill the uncertainty relation. The variance  $\Delta x \Delta p_x$  of two neighboring eigenfunctions is separated by  $\hbar/2$ , i.e., each level fills a volume of  $h^3$  in phase space. if a system is in its ground state , the phase space is densely filled up to a maximum value in coordinate and momentum space, in which there has no hole. This is the property of the ground state. To initialize the ground state of nucleus A, one first determines the position of the nucleons in a sphere of the radius  $r = 1.12A^{1/3}$  fm drawing random numbers but rejecting those which would position the centers of two nucleons closer than  $r_{min}=1.5$  fm. The next step is to determine the local potential  $U(r)$  generated by all the other nucleons at the centers of the Gaussians. The local Fermi momentum is determined by the relation  $p_F(r_{i0}) = \sqrt{2mU(r_{i0})}$ , where  $U(r_{i0})$  is the potential energy of particle i. Finally the momenta of all particles are chosen randomly between zero and the local Fermi momentum. We then reject all random numbers which yield two particles closer in phase space than  $(r_i - r_j)^2(p_i - p_j)^2 = d_{min}$  . Typically only 1 out of 50,000 initializations is accepted under the present criteria. The computer time required for the initialization is short compared to the time needed for the propagation.

## 2.2 Propagation

Nuclei which have been successfully initialized are then boosted towards each other with the proper center of mass velocity using relativistic kinematics. The centers of projectile and target move along Coulomb trajectories up to a distance of 2 fm between the surface of projectile and target. Because we keep the width of the Gaussians fixed, the time evolution of the A-body distribution is determined by the motion of the centroids of the Gaussians ( $\mathbf{r}_{i0}, \mathbf{p}_{i0}$ ), which are propagated by the Poisson brackets

$$\dot{p}_{i0} = \{r_{i0}, H\} = \{r_{i0}, T + U\}, \quad (2.5)$$

and

$$\dot{r}_{i0} = \{p_{i0}, H\} = \{p_{i0}, T + U\}. \quad (2.6)$$

Here T is the total kinetic energy and U is the total potential energy of all nucleons. These differential equations are solved using an Eulerian integration routine with a fixed time step  $\Delta t$ ,

$$p_{i0}(n+1) = p_{i0}(n) - \nabla_{r_{i0}} U_i \left( n + \frac{1}{2} \right) \Delta t, \quad (2.7)$$

$$r_{i0} \left( n + \frac{1}{2} \right) = r_{i0} \left( n - \frac{1}{2} \right) + \frac{p_{i0}(n)}{[p_{i0}(n)^2 + m_i^2]^{1/2}} \Delta t + \nabla_{p_{i0}} U_i \left( n - \frac{1}{2} \right) \Delta t. \quad (2.8)$$

The particles interact via two and three body interactions. This is essential if the fluctuations and correlations are to be preserved. We assume that the short range interactions between the nucleons accounts for the bulk properties. One uses here a local Skyrme-type interaction supplemented by a long range Yukawa interaction which is necessary to reproduce surface and an Coulomb interaction. The total static interaction is given by

$$V^{tot} = V^{loc} + V^{Yuk} + V^{Coul}, \quad (2.9)$$



where the different terms are

$$V^{loc} = t_1\delta(\mathbf{r}_1 - \mathbf{r}_2) + t_2\delta(\mathbf{r}_1 - \mathbf{r}_2)\delta(\mathbf{r}_1 - \mathbf{r}_3), \quad (2.10)$$

$$V^{Yuk} = t_3 \frac{e^{-|\mathbf{r}_1 - \mathbf{r}_2|/m}}{|\mathbf{r}_1 - \mathbf{r}_2|/m} \quad (2.11)$$

with  $m = 0.8$  fm and  $t_3 = -6.66$  MeV. These parameters give the best preservation of the nuclear surface.

The total energy  $H_i$  of particle  $i$  is the sum of kinetic and potential energies,

$$H_i = T_i + U_i = T_i + \frac{1}{2} \sum_{j \neq i} U_{ij}^{(2)} + \frac{1}{3!} \sum_{jk \neq i} U_{ijk}^{(3)}. \quad (2.12)$$

$T_i$  refers to the kinetic energy of particle  $i$  and the potentials are given as

$$\begin{aligned} U_i^{(2)}(t) &= \sum_{j \neq i} U_{ij}^{(2)} = \sum_{j \neq i} \int f_i(\mathbf{r}_i, \mathbf{p}_i, t) f_j(\mathbf{r}_j, \mathbf{p}_j, t) V^{(2)}(\mathbf{r}_i - \mathbf{r}_j) d^3\mathbf{r}_i d^3\mathbf{p}_i d^3\mathbf{r}_j d^3\mathbf{p}_j \\ &= U_{i loc}^{(2)} + U_{i Yuk}^{(2)} + U_{i Coul}^{(2)}, \end{aligned} \quad (2.13)$$

where

$$U_{i loc}^{(2)} = t_1 \rho(\mathbf{r}_{i0}), \quad (2.14)$$

where the interaction density  $\rho(\mathbf{r}_{i0})$  is

$$\rho(\mathbf{r}_{i0}) = \frac{1}{(4\pi L)^{3/2}} \sum_{j \neq i} e^{(\mathbf{r}_{i0} - \mathbf{r}_{j0})^2 / 4L}. \quad (2.15)$$

The interaction density has twice the width of the single particle density.

$$\begin{aligned} U_{i Yuk}^{(2)} &= \sum_{j \neq i} U_{ij Yuk}^{(2)} \\ &= t_3 \sum_{j \neq i} \frac{e^{L/m^2}}{r_{ij}/2m} \left\{ e^{-r_{ij}/m} \left[ 1 - \Phi \left( \frac{\sqrt{L}}{m} - \frac{r_{ij}}{2\sqrt{L}} \right) \right] \right. \\ &\quad \left. - e^{r_{ij}/m} \left[ 1 - \Phi \left( \frac{\sqrt{L}}{m} + \frac{r_{ij}}{2L} \right) \right] \right\} \end{aligned} \quad (2.16)$$

Here  $\Phi(x)$  is the error function.  $U_{iCoul}^{(2)}$  is the Coulomb energy.

The three body potential with  $\nu = 2$  is given by

$$\begin{aligned}
U_i^{(3)} &= \sum_{j,k;j,k \neq i,k \neq j} U_{ijk}^{(3)} \\
&= t_2 \sum_{j,k;j,k \neq i,k \neq j} \int f_i(\mathbf{r}_i, \mathbf{p}_i, t) f_j(\mathbf{r}_j, \mathbf{p}_j, t) f_k(\mathbf{r}_k, \mathbf{p}_k, t) \\
&\quad \times V^{(3)} d^3 \mathbf{r}_i d^3 \mathbf{p}_i d^3 \mathbf{r}_j d^3 \mathbf{p}_j d^3 \mathbf{r}_k d^3 \mathbf{p}_k \\
&= \frac{t_2}{(2\pi L)^3 3^{3/2}} \\
&\quad \times \sum_{j,k;j,k \neq i,k \neq j} \exp\{[(\mathbf{r}_{i0} - \mathbf{r}_{j0})^2 + (\mathbf{r}_{i0} - \mathbf{r}_{k0})^2 + (\mathbf{r}_{j0} - \mathbf{r}_{k0})^2]/6L\} \\
&\approx \frac{t_2}{(2\pi L)^3 3^{3/2}} \sum_{j,k;j,k \neq i} \exp[(\mathbf{r}_{i0} - \mathbf{r}_{j0})^2 + (\mathbf{r}_{i0} - \mathbf{r}_{k0})^2]/4L \\
&\approx \frac{t_2 (4\pi L)^{3\nu/2}}{(2\pi L)^{3(\nu-1)/2} (\nu+1)^{3/2}} \rho_i^\nu(\mathbf{r}_{i0}) \tag{2.17}
\end{aligned}$$

The expectation value of the total energy is

$$E = \sum_i [T_i + \frac{1}{2} U_i^{(2)} + \frac{1}{3!} U_i^{(3)}], \tag{2.18}$$

where the upper index refers to the two and three body interaction, respectively.

Next we have to determine the parameters  $t_1 - t_3$ . We start out from the observation that in nuclear matter, where the density is constant,  $U^{(2)}$  is directly proportional to  $\rho/\rho_0$ . In spin saturated nuclear matter the three body interaction is equivalent to a density dependent two body interaction. If we assume that the density does not vary substantially over the distance of the two body interaction  $U^{(3)}$  is then proportional to  $(\rho/\rho_0)^2$ . This observation allows to relate our parameters to nuclear matter properties. In nuclear matter our potential has the form

$$U^{loc} = \alpha \left( \frac{\rho}{\rho_0} \right) + \beta \left( \frac{\rho}{\rho_0} \right)^2 \tag{2.19}$$

This potential has two free parameters which can be fixed by the requirement that at normal nuclear matter density the average binding energy is 16 MeV

and the total energy has a minimum at  $\rho_0$ . The adjustment of the two parameters fixes the compressibility as well. In order to investigate the influence of different compressibilities one can generalize the potential to

$$U^{loc} = \alpha \left( \frac{\rho}{\rho_0} \right) + \beta \left( \frac{\rho}{\rho_0} \right)^\gamma \quad (2.20)$$

Now we have in addition a third parameter which allows to fix the compressibility independently from the other quantities. This generalization can be translated back to the nucleon-nucleon potential in a unique way by identifying  $\nu$  with  $\gamma$ . The parameter  $\alpha$  contains contributions from the local two body interaction as well as from the Yukawa potential. The latter can be obtained by the Taylor expansion

$$\begin{aligned} U_{Yuk} &\sim \int d^3\mathbf{r} \int d^3\mathbf{r}' \frac{e^{-|\mathbf{r}-\mathbf{r}'|/m}}{|\mathbf{r}-\mathbf{r}'|/m} \rho(\mathbf{r})\rho(\mathbf{r}') \\ &= 4\pi m^3 \left\{ \int d^3\mathbf{r} \rho^2(\mathbf{r}) + m^2 \int d^3\mathbf{r} [\rho(\mathbf{r})\nabla^2\rho(\mathbf{r})] \right\} \end{aligned} \quad (2.21)$$

Here  $\alpha$  is given by

$$\alpha \sim t_1 - 4\pi m^3 t_3. \quad (2.22)$$

The relative weight between  $t_1$  and  $t_2$  as well as the parameter  $m$  are adjusted to obtain reasonable binding energies of finite nuclei. One finds that  $t_2 = 10$  MeV and  $m = 0.8$  fm give  $E/A = 6-14$  MeV for  $A = 7-200$ . The coefficients of proportionality between  $\alpha$  and  $t_1$  and  $\beta$  and  $t_2$ , respectively, are determined numerically.

However, we want to stress that for the actual propagational ways the explicit two and three body interactions are used and not the nuclear matter potentials. This is important since the equivalence of both is only true in nuclear matter, not in finite nuclei. This equivalence can be used to connect the parameters  $t_1 - t_3$  with nuclear matter properties, i.e., the nuclear equation of state. For this reason, our approach allows to investigate in detail how a given nuclear equation

of state shows up indifferent observable in a heavy ion reaction. In nuclear matter our two and three body interaction are up to small correction equivalent to a density dependent interaction of the form.

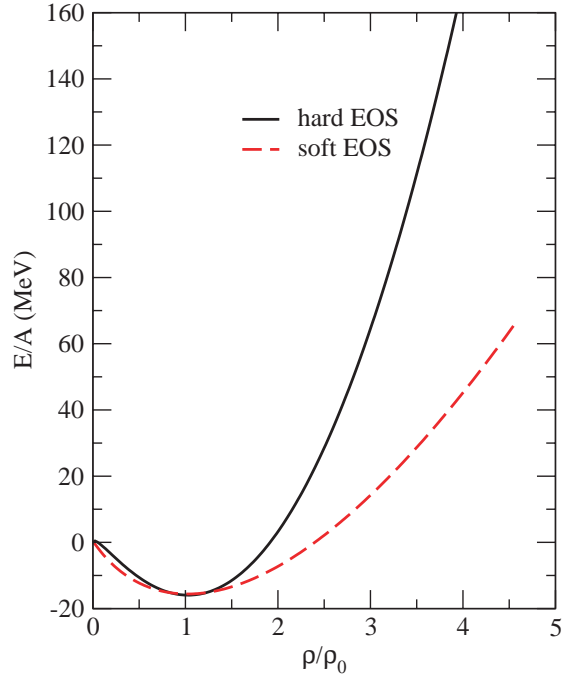


**Figure 2.1** Equation of state. The density dependence of the energy per particle in nuclear matter at temperature  $T = 0$  is displayed for two different sets of parameters

In Fig. (2.1) we display the density dependence of the ground state energy per particle in nuclear matter for two different sets of parameters. The parameters Eq. (2.20) are given in Table (2.1).

This form of the nucleon-nucleon potential can easily be supplemented by a momentum dependent interaction (H,S) (Aichelin, 1991; Aichelin and Stoecker, 1986; Bass, 1998). For a given compressibility this does not change the energy in nuclear matter up to 4 times nuclear matter density, but has important consequences concerning the dynamics of a heavy ion reaction. Therefore in the present

**Table 2.1** The parameters of Eq. (2.20) for the hard (H) and the soft (S) EOS.

K	$\alpha$	$\beta$	$\gamma$	EOS
200 MeV	-356 MeV	303 MeV	$\frac{7}{6}$	S
380 MeV	-124 MeV	70.5 MeV	2	H

calculations we apply momentum dependent Skyrme force.

### 2.3 Collision

The scattering of nucleons in nuclear matter in the low density expansion is described in terms of the reaction  $g$  matrix (Jeukenne, Lejeune and Mahaux, 1976).

$$g(E) = V + V \frac{Q}{E - e + i\epsilon} g(E), \quad (2.23)$$

where the Pauli operator  $Q$  projects on unoccupied states only and  $e$  is the energy of the intermediate state,  $e = p_1^2/2m + p_2^2/2m + U(p_1) + U(p_2)$ .

In the QMD model simulations were stricted to binary collisions (two-body level). The collisions are performed in a point particle sense in a similar way as in the VUU or cascade code (Cugnon, 1980). Two particles collide if their minimum distance, i.e. the minimum relative distance of the centroids of the Gaussians during their motion, in their CM frame fulfills the requirement,

$$d \leq d_0 = \sqrt{\frac{\sigma_{tot}}{\pi}}. \quad (2.24)$$

Beside the parameters describing the NN potential, the cross sections are another major part of the model. In principle, both quantities are connected and can be deduced from Brueckner theory. QMD calculations using consistently derived cross-sections and potentials from the local phase space distributions

have been discussed (Jaenicke, Aichelin, Ohtsuka, Lindenc and Amand Faessler, 1992). Such simulations are time-consuming since the cross-sections and potentials do explicitly depend on the local phase space population. Within the framework of using free cross section one may parameterize the cross section of the processes to fit the experimental data if available. For unknown cross sections isospin symmetry and time reversibility is assumed.

The cross section is reduced to an effective cross section by the Pauli blocking. For each collision the phase space densities in the final states are checked in order to assure that the final distribution in phase space is in agreement with the Pauli principle ( $P \leq 1$ ). Phase space in the QMD model is not discretized into elementary cells as in one-body models like the VUU. In order to obtain smooth distribution functions the following procedure is applied: The phase space density  $P'_i$  at the final states  $1'$  and  $2'$  is measured and interpreted as a blocking probability. Thus, the collision is only allowed with a probability of  $(1-P'_1)(1-P'_2)$ . If the collision is not allowed, the particles remain at their original momenta.

One stresses that our QMD model code has recently been extended (Uma Maheswari, Fuchs, Amand Faessler, Sehn, Kosov and Wang, 1998; Shekhter, Christian, Amand Faessler and Krivoruchenko, 2003) to include all nuclear resonances with masses below 2 GeV, which include 11  $N^*$  and 10  $\Delta$  resonances. The corresponding masses and decay widths are listed in Tables (2.2) and (2.3).

**Table 2.2** List of  $N^*$  resonances which are included in the QMD model. The table shows the resonance masses and the total and partial widths of the included decay channels in MeV. For details, please see the work (Shekgter, Christian, Amand Faessler and Krivoruchenko, 2003).

Resonance	Mass [MeV]	$\Gamma_{tot}(MeV)$	$N_{\pi\pi}$	$\Delta_{1232\pi}$	$N_{1440\pi}$
$N_{1440}$	1440	200	10	50	-
$N_{1520}$	1520	125	18.75	31.25	-
$N_{1535}$	1535	150	7.5	-	7.5
$N_{1650}$	1650	150	7.5	15	7.5
$N_{1675}$	1675	140	77	-	-
$N_{1680}$	1860	120	18	-	-
$N_{1700}$	1700	100	45	35	-
$N_{1710}$	1710	110	22	22	11
$N_{1720}$	1720	184(150)	67.5	15	-
$N_{1900}$	1870	500	-	25	-
$N_{1990}$	1990	550	137.5	165	82.5

**Table 2.3** List of  $\Delta$  resonances which are included in the QMD model. The table shows the resonance masses, and the total and partial widths of the included decay channels in MeV. For details, please see the work (Shekgter, Christian, Amand Faessler and Krivoruchenko, 2003).

Res.	Mass [MeV]	$\Gamma_{\text{tot}}$ [MeV]	$N\rho$	$N\pi$	$\Delta_{1232\pi}$	$N_{1440\pi}$	
$\Delta_{1232}$	1232	115	$\sim 0$	(-)	115	-	-
$\Delta_{1600}$	1700	200	-	(-)	30	110	60
$\Delta_{1620}$	1675	180	16.4	(-)	45	108	27
$\Delta_{1700}$	1750	300	47.7	(30)	60	165	45
$\Delta_{1900}$	1850	240	-	(36)	72	72	60
$\Delta_{1905}$	1880	363 (280)	307.3	(168)	56	28	28
$\Delta_{1910}$	1900	250	-	(100)	87.5	37.5	25
$\Delta_{1920}$	1920	150	-	(45)	22.5	45	37.5
$\Delta_{1930}$	1930	250	-	(62.5)	50	62.5	75
$\Delta_{1950}$	1950	250	-	(37.5)	112.5	50	50



We take the iso-spin dependent production cross sections  $\sigma^{NN \rightarrow NR}$  for the  $\Delta(1232)$  and the  $N^*(1440)$  resonances from (Shekhter, Christian, Amand Faessler and Krivoruchenko, 2003). These cross sections are determined within the framework of a one-boson-exchange model. For the higher lying resonances parameterizations for the production cross-section are taken from different sources (Bass, 1998; Teis, 1997). The following baryon-baryon collisions are included: all elastic channels,  $NN \rightarrow NN^*$ ,  $NN \rightarrow N\Delta^*$ ,  $NN \rightarrow \Delta_{1232}N^*$ ,  $NN \rightarrow \Delta_{1232}\Delta^*$  and  $NR \rightarrow NR'$ , where  $\Delta^*$  denotes all higher lying  $\Delta$ -resonances. Elastic scattering is considered on the same footing for all the particles involved. Matrix elements for elastic reactions are assumed to be the same for nucleons and nucleonic resonances. Thus elastic  $NR$  and  $RR$  cross sections are determined from the elastic  $pp$  or  $np$  cross sections, depending on the total charge. Inelastic collisions are considered according to the expression (Bass, 1998).

$$\sigma_{1,2 \rightarrow 3,4} \sim \frac{\langle p_f \rangle}{p_i s} |\mathcal{M}(m_3, m_4)|^2 \quad (2.25)$$

$p_i$  and  $\langle p_f \rangle$  are the momenta of incoming and outgoing particles in the center of mass frame. In the case that final states are resonances, the phase space has to be averaged over the corresponding spectral function

$$\langle p_f \rangle = \int p(\sqrt{s}, m_N, \mu) dW_{R'}(\mu) \quad (2.26)$$

with  $dW_{R'}(\mu)$  given by the corresponding Breit-Wigner distribution.

$$dW_R(\mu) = \frac{1}{\pi} \frac{\mu \Gamma^R(\mu) d\mu^2}{(\mu^2 - m_R^2)^2 + [\mu \Gamma_{tot}^R(\mu)]^2}, \quad (2.27)$$

where  $\mu$  and  $m_R$  are the running and pole masses, respectively.  $\Gamma(\mu)$  is the mass dependent resonance width. In the general case that both final states in Eq. (2.25) are resonances the averaging of  $p_f$  is performed over both resonances,

$$\langle p_f \rangle = \int p(\sqrt{s}, \mu, \mu') dW_R(\mu) dW_{R'}(\mu') \quad (2.28)$$

The integrations are performed over kinematically defined limits.  $\mathcal{M}$  in Eq. (2.25) is the matrix element of the cross-section and the proportionality sign accounts for possible overall isospin coefficients. For most of the cases we use expressions for the matrix elements from (Bass, 1998). However, parameterizations of the matrix elements are given in (Teis, 1997). we make use of these expressions. This is in particular the case for reactions where resonances contribute to the dilepton yield. e.g. the cross-section for the reactions  $NR \rightarrow NR'$  is determined from the known channels  $NN \rightarrow NR$  and  $NN \rightarrow NR'$  by

$$\sigma_{NR \rightarrow NR'} = I \frac{0.5(|\mathcal{M}_{NN \rightarrow NR}|^2 + |\mathcal{M}_{NN \rightarrow NR'}|^2)2(2J_{R'} + 1)}{16\pi p_i s} \langle p_f \rangle . \quad (2.29)$$

In Eq. (2.29)  $I$  is an isospin coefficient, depending on the resonances' types, and  $J_{R'}$  denotes the spin of  $R'$ .

For all resonances we use mass-dependent widths in expressions Eq. (2.29-2.28), namely

$$\Gamma(\mu) = \Gamma_R \left( \frac{p}{p_r} \right)^3 \left( \frac{p_r^2 + \delta^2}{p^2 + \delta^2} \right)^2 . \quad (2.30)$$

In Eq. (2.30)  $p$  and  $p_r$  are the c.m. momenta of the pion in the resonance rest frame evaluated at the running and the resonance pole mass, respectively.  $\delta = 0.3$  is chosen for the  $\Delta_{1232}$  and  $\delta = \sqrt{(m_R - m_N - m_\pi)^2 + \Gamma^2/4}$  for the rest of the resonances. The inclusive  $\pi^- p$  and  $\pi^+ p$  cross sections are shown in Fig. (2.2). The fit to the data including the sum over all resonances is of similar quality as in (Teis, 1997; Bass, 1998) and reproduces the absorption cross section up to pion laboratory momenta of 1-1.5 GeV. At higher energies string excitations start to play a role (Bass, 1998). Backward reactions, e.g.  $NR \rightarrow NN$ , are treated by detailed balance

$$\sigma_{3,4 \rightarrow 1,2} \sim \frac{|p_{1,2}|^2}{|p_{3,4}|^2} \sigma_{1,2 \rightarrow 3,4}, \quad (2.31)$$

where the proportionality sign is due to overall isospin factors. The expressions

for the momenta of incoming (outgoing) particles are calculated according to Eqs. (2.29) and (2.28), respectively. Pion-baryon collisions are standardly treated as two-stage processes, i.e. first the pion is absorbed by a nucleon or a baryonic resonance forming a new resonance state with subsequent decay. The pion absorption by nucleons is treated in the standard way (Uma Maheswari, Fuchs, Amand Faessler, Sehn, Kosov and Wang, 1998; Teis, 1997; Bass, 1998) and the pion absorption by resonances is proportional to the partial decay width of the reverse process (Teis, 1997).

$$\sigma_{\pi R \rightarrow R'} = \frac{2J_{R'} + 1}{(2S_a + 1)(2S_b + 1)} \frac{4\pi}{p_i^2} \frac{s(\Gamma_{R' \rightarrow R\pi})^2}{(s - m_{R'}^2)^2 + s\Gamma_{R'}^2} . \quad (2.32)$$

The decay of baryonic resonances is treated as proposed in (Danielewicz and Pratt, 1996; Larionov, Effenberger, Leupold and Mosel, 2002), i.e. the resonance life time is given by the spectral function

$$\tau_R(\mu) = 4\pi\mu \frac{dW_R(\mu)}{d\mu^2} . \quad (2.33)$$

Here we use constant widths when considering resonance decays. The decay channels, which are taken into account, are listed in Tables (3) and (4) together with their corresponding branching ratios. For the mass systems under consideration pion multiplicities are reasonably well reproduced by the present description, e.g. inclusive  $\pi^+$  cross sections in  $C + C$  reactions were recently measured by the KaoS Collaboration and the experimental results can be reproduced by the present description within error bars (Fuchs, 2006).

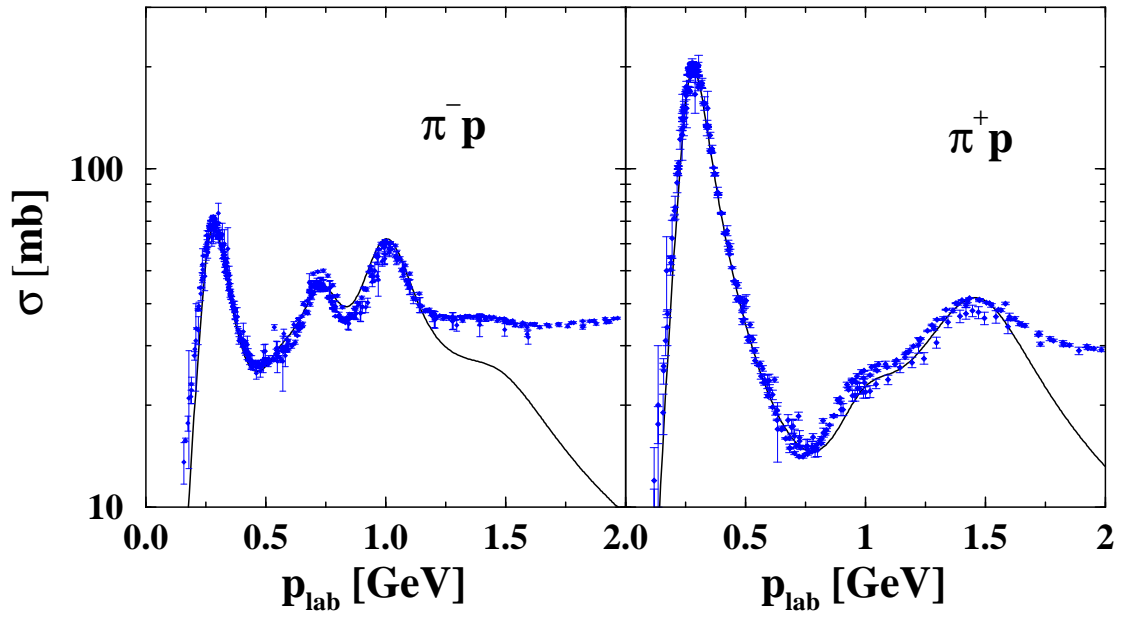


**Figure 2.2** Inclusive  $\pi^-p$  and  $\pi^+p$  cross sections obtained by the sum over all resonances which are taken into account in the present description

# CHAPTER III

## KAON MESON PRODUCTION IN HEAVY ION COLLISIONS

### 3.1 Kaon covariant dynamics

Properties of kaons in dense hadronic matters are very important for a better understanding of both the possible restoration of chiral symmetry in dense hadronic matters and the properties of nuclear matters at high densities.

Due to its relativistic origin, the kaon mean field has a typical relativistic-scalar-vector-type structure. For the nucleons such a structure is well known from Quantum Hadron Dynamics (Serot and Walecka, 1986). This decomposition of the mean field is most naturally expressed by an absorption of the scalar and vector parts into effective masses and momenta, respectively, leading to a formalism of quasifree particles inside the nuclear medium (Serot and Walecka, 1986).

From the chiral Lagrangian the field equations for the  $K^\pm$  mesons are derived from the Euler-Lagrange equations (Li, Ko and Bao-An Li, 1995; Li and Ko, 1995)

$$[\partial_\mu \partial^\mu \pm \frac{3i}{4f_\pi^{*2}} j_\mu \partial^\mu + (m_K^2 - \frac{\sum_{KN}}{f_\pi^{*2}} \rho_s)] \phi_{K^\pm}(x) = 0. \quad (3.1)$$

Here the mean-field approximation has already been applied. In Eq. (3.1)  $\rho_s$  is the baryon scalar density,  $j_\mu$  is the baryon four-vector current,  $f_\pi^*$  is the in-medium pion decay constant. Introducing the kaonic vector potential

$$V_\mu = \frac{3}{8f_\pi^{*2}} j_\mu, \quad (3.2)$$

Eq. (3.1) can be rewritten in the form (Fuchs, Kosov, Faessler, Wang and Waindzo-  
zoch, 1998; Zheng, Fuchs, Faessler, Shekhter, Yan and Kobdaj, 2004)

$$[(\partial_\mu \pm iV_\mu)^2 + m_K^{*2}] \phi_{K^\pm}(x) = 0. \quad (3.3)$$

Thus, the vector field is introduced by minimal coupling into the Klein-Gordon equation. The effective mass  $m_K^*$  of the kaon is then given by (Schaffner, Bondorf and Mishustin, 1997; Fuchs, Kosov, Faessler, Wang and Waindzo-  
zoch, 1998; Fuchs, Faessler, Wang and Gross-Boelting, 1999; Fuchs, Faessler, Zabrodin and Zheng, 2001; Zheng, Chu, Fuchs, Faessler, Xiao, Hua and Yan, 2002; Zheng, Fuchs, Faessler, Shekhter, Yan and Kobdaj, 2004)

$$m_K^* = \sqrt{m_K^2 - \frac{\sum_{KN}}{f_\pi^{*2}} \rho_s + V_\mu V^\mu}. \quad (3.4)$$

Due to the bosonic character, the coupling of the scalar field to the mass term is no longer linear as for the baryons but quadratic and contains an additional contribution originating from the vector field. The effective quasiparticle mass defined by Eq. (3.4) is a Lorentz scalar and is equal for  $K^+$  and  $K^-$ . In nuclear matter at rest the spatial components of the vector potential vanish, i.e.,  $V = 0$ , and Eq. (3.3) reduces to the expression already given in (Li, Ko and Bao-An Li, 1995; Li and Ko, 1995). However, Eq. (3.3) generally account for the correct Lorentz properties which are not obvious from the standard treatment of the kaon mean field (Li, Ko and Bao-An Li, 1995; Li and Ko, 1995; Ko and Li, 1996; Bratkovskay, Cassing and Mosel, 1998; Li, Lee and Brown, 1997; Li, Ko and Bao-An, 1997).

The covariant equations of motion are obtained in the classical (test particle) limit from the relativistic transport equation for the kaons which can be derived from Eq. (3.3). They are analogous to the corresponding relativistic equa-

tions for baryons and read (Fuchs, Kosov, Faessler, Wang and Waindzoeh, 1998; Zheng, Fuchs, Faessler, Shekhter, Yan and Kobdaj, 2004)

$$\frac{dq^\mu}{d\tau} = \frac{k^{*\mu}}{m_K^*}, \quad \frac{dk^{*\mu}}{d\tau} = \frac{k_\nu^*}{m_K^*} F^{\mu\nu} + \partial^\mu m_K^*. \quad (3.5)$$

Here  $q^\mu = (t, \mathbf{q})$  are the coordinates in Minkowski space and  $F^{\mu\nu} = \partial^\mu V^\nu - \partial^\nu V^\mu$  is the field strength tensor for  $K^+$ . For  $K^-$  where the vector field changes sign. The equation of motion are identical, however,  $F^{\mu\nu}$  has to be replaced by  $-F^{\mu\nu}$ . The structure of Eq. (3.5) may become more transparent considering only the spatial components

$$\frac{d\mathbf{k}^*}{dt} = -\frac{m_K^*}{E^*} \frac{\partial m_K^*}{\partial \mathbf{q}} \mp \frac{\partial V^0}{\partial \mathbf{q}} \pm \frac{\mathbf{k}^*}{E^*} \times \left( \frac{\partial}{\partial \mathbf{q}} \times \mathbf{V} \right), \quad (3.6)$$

where the upper (lower) signs refer to  $K^+$  and  $K^-$ . The term proportional to the spatial component of the vector potential gives rise to a momentum dependence which can be attributed to a Lorentz force, i.e., the last term in Eq. (3.6). Such a velocity dependent ( $v = \mathbf{k}^*/E^*$ ) Lorentz force is a genuine feature of relativistic dynamics as soon as a vector field is involved.

If the equation of motion are, however, derived from a static potential

$$U(\rho, \mathbf{k}) = \omega(\rho, \mathbf{k}) - \omega_0(\mathbf{k}) = \sqrt{\mathbf{k}^2 + m_k^2 - \frac{\Sigma_{KN}}{f_\pi^{*2}} \rho_s + V_0^2} \pm V_0 - \sqrt{\mathbf{k}^2 + m_K^2} \quad (3.7)$$

as given in (Zheng, Fuchs, Faessler, Shekhter, Yan and Kobdaj, 2004), the Lorentz-force (LF) like contribution is missing. Non-covariant treatments are formulated in terms of canonical momenta  $k$  instead of kinetic momenta  $k^*$  and then the equations of motion read

$$\frac{d\mathbf{k}}{dt} = -\frac{m_K^*}{E^*} \frac{\partial m_K^*}{\partial \mathbf{q}} \mp \frac{\partial V^0}{\partial \mathbf{q}} \pm v_i \frac{\partial \mathbf{V}_i}{\partial \mathbf{q}}, \quad (3.8)$$

where  $v = \mathbf{k}^*/E^*$  the kaon velocity.

In order to account for energy-momentum conservation it is useful to formulate the mass-shell condition, Eq. (3.3), in terms of the canonical momenta

$$0 = k_\mu^{*2} - m_K^{*2} = k_\mu^2 - m_K^2 - 2m_K U_{opt}, \quad (3.9)$$

with

$$U_{opt}(\rho, \mathbf{k}) = -\Sigma_S + \frac{1}{m_K} k_\mu V^\mu + \frac{\sum_S^2 - V_\mu^2}{2m_K}, \quad (3.10)$$

Here we introduced the total scalar kaon self-energy  $\Sigma_S = m_K^* - m_K$ . Since  $U_{opt}$  is a Lorentz scalar it can also be absorbed into an effective mass

$$\tilde{m}_K(\rho, \mathbf{k}) = \sqrt{m_K^2 + 2m_K U_{opt}(\rho, \mathbf{k})}, \quad (3.11)$$

which sets the canonical momenta on the mass-shell

$$0 = k_\mu^{*2} - m_K^{*2} = k_\mu^2 - \tilde{m}_K^2. \quad (3.12)$$

By definition  $\tilde{m}_K$  is a scalar but in contrast to  $m_K^*$  whose analogy is the Dirac mass in the case of nucleons.  $\tilde{m}_K$  absorbs the full optical potential and corresponds at zero momentum to the energy  $\omega$ .

## 3.2 Kaon production in the QMD model

Kaons have been considered as one of the best probes to study dense and hot nuclear matters formed in relativistic heavy ion collisions. In particular at incident energies below the production thresholds in free space  $K^+$  mesons are created in the early and high density phase of such reactions.  $K^+$  meson cannot be absorbed by the surrounding nucleons due to the strangeness conservation. This results in a rather long mean free path of about 7 fm in nuclear matters and makes it a suitable penetrating probe for the dense fireball produced in heavy ion reactions.



In the kaon production the baryon dynamics are treated within the framework of the QMD model. One uses the standard momentum dependent Skyrme interactions corresponding to a soft/hard nuclear equation of state ( $K=200/380$  MeV) for the baryon interactions. For the determination of the kaon mean field we adopt the corresponding covariant scalar-vector description of the nonlinear  $\sigma\omega$  model. Following Brown and Rho, we use  $\sum_{KN} = 450$  MeV,  $f_{\pi}^{*2} = 0.6f_{\pi}^2$  for the vector field and  $f_{\pi}^{*2} = f_{\pi}^2$  for the scalar part given by  $-\Sigma_{KN}/f_{\pi}^{*2}\rho_s$ . This accounts for the fact that the enhancement of the scalar part using  $f_{\pi}^{*2}$  is compensated by higher-order correction in the chiral expansion (Brown and Pho, 1996). This parametrization is denoted as Brown and Rho parametrization (BRP), which has already been used in our previous investigations (Fuchs, Kosov, Faessler, Wang and Waindzoeh, 1998; Fuchs, Faessler, Zabrodin and Zheng, 2001).

The  $K^+$  creation mechanism is treated as described in the work (Fuchs, Faessler, Zabrodin and Zheng, 2001) where one uses the improved cross section of the works (Sibirtsev, 1995; Tsushima, Sibirtsev, Thomas and Li, 1999; Tsushima, Sibirtsev, Thomas and Li, 1999) for the baryon induced  $K^+$  creation channels  $BB \rightarrow BYK^+$  see Fig. (3.1) and the one of the works (Tsushima, Huang and Faessler, 1995) for the pion induced channels  $\pi B \rightarrow YK^+$ . Here  $B$  stands for a baryon which can be either a nucleon or a nucleon resonance  $N, \Delta$ , and  $N^*$ , and  $Y$  for a  $\Lambda$  or a  $\Sigma$  hyperon. The kaon production is treated perturbatively and does generally not affect the reaction dynamics (Ko and Li, 1996; Fuchs, Faessler, Zabrodin and Zheng, 2001).

The shift of the production thresholds of the kaons by the in-medium potentials are taken into account as described in (Fuchs, Faessler, Zabrodin and Zheng, 2001). The threshold condition for  $K^+$  production in baryon induced reactions

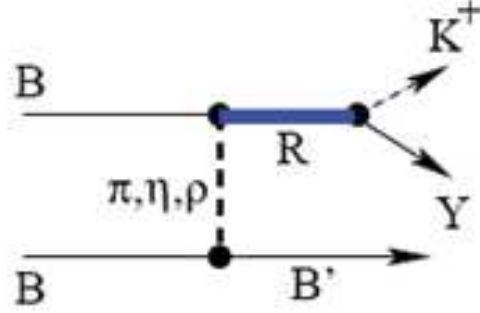


**Figure 3.1** Diagrammatic representation of the reaction  $BB \rightarrow BYK^+$

reads then

$$\sqrt{s} \geq \tilde{m}_B + \tilde{m}_Y + \tilde{m}_K, \quad (3.13)$$

where  $\sqrt{s}$  is the center-of-mass energy of the colliding baryons.  $\tilde{m}_K$  is given by Eq. (3.11). The momenta of the outgoing particles are distributed according to the three-body phase space

$$d\Phi_3(\sqrt{s}, \tilde{m}_B, \tilde{m}_Y, \tilde{m}_K) = d\Phi_2(\sqrt{s}, \tilde{m}_B, M) dM^2 \Phi_2(M, \tilde{m}_Y, \tilde{m}_K). \quad (3.14)$$

The two-body phase space in Eq. (3.14) has the form

$$\Phi_2(\sqrt{s}, m_1, m_2) = \frac{\pi \rho^*(\sqrt{s}, m_1, m_2)}{\sqrt{s}}, \quad (3.15)$$

where

$$p^*(\sqrt{s}, m_1, m_2) = \frac{\sqrt{(s - (m_1 + m_2)^2)(s - (m_1 - m_2)^2)}}{2\sqrt{s}} \quad (3.16)$$

is the momentum of the particles 1 and 2 in the center of mass c.m. frame. Eq. (3.14) corresponds to a distribution of the particle momenta according to an isotropic three-body phase space. However, in (Li, Lee and Brown, 1997; Li, Ko and Li, 1997) a parametrization of the form

$$d\Phi_3(\sqrt{s}, \tilde{m}_B, \tilde{m}_Y, \tilde{m}_K) = dW_K(\sqrt{s}, \tilde{m}_B, \tilde{m}_Y, M_K) dM_K^2 \Phi_2(\sqrt{s} - M_K, \tilde{m}_Y, \tilde{m}_B), \quad (3.17)$$

has been suggested where the kaon momentum  $p$  is distributed according to

$$dW_K \simeq \left( \frac{p}{p_{\max}} \right)^3 \left( 1 - \frac{p}{p_{\max}} \right)^2, \quad (3.18)$$

with  $p_{\max} = p^*(\sqrt{s}, \tilde{m}_B + \tilde{m}_Y, \tilde{m}_K)$  the maximal kaon momentum in the BB c.m. frame.  $M_K = \sqrt{p^2 + \tilde{m}_K^2}$  in Eq. (3.17). The parametrization of Eq. (3.17) has been motivated by analyzing corresponding  $pp \rightarrow p\Lambda K^+$  data (Li, Lee and Brown, 1997; Li, Ko and Li, 1997) and shifts the kaon spectrum to lower momenta compared to an ideal three-body phase space. The optical potentials of the baryons which enter via  $\tilde{m}_B, \tilde{m}_Y$  are taken from the soft/hard EOS versions of the  $\sigma\omega$  model (Ko and Li, 1996). The hyperon fields are thereby scaled according to SU(3) symmetry  $U_{opt}^Y = \frac{2}{3}U_{opt}^B$ . Since the  $\tilde{m}'s$  depend on the final state momenta the determination of  $d\Phi_3$  is a self-consistency problem which is solved by iteration. The same procedure is applied to the two-body-phase space in pion induced reactions. The rescattering of the  $K^+$  mesons with baryons and the Coulomb interaction are taken into account. The electromagnetic interaction is treated analogously to the strong interaction, i.e., by adding  $F_{el}^{\mu\nu} = \partial^\mu A^\nu - \partial^\nu A^\mu$  given by the electromagnetic vector potential to Eq. (3.5).

### 3.3 Results and discussions

In order to study first the influence of covariant dynamics on the  $K^+$  in-plane flow we consider the 1.93 A GeV  $^{58}\text{Ni} + ^{58}\text{Ni}$  collisions at impact parameter  $b \leq 4$  fm, corresponding to the FOPI centrality. Shown in Fig. (3.2) is the  $K^+$  transverse flow as a function of the scaled rapidity  $Y^0$  ( $Y^0 = Y_{lab}/Y_{CM} - 1$ ) in 1.93 A GeV  $^{58}\text{Ni} + ^{58}\text{Ni}$  reactions. In the figure the full squares represent the '95 data set from FOPI (old data) (Ritman and FOPI Collaboration, 1995), and the full and open circles stand for the '99 data from FOPI with improved statistics

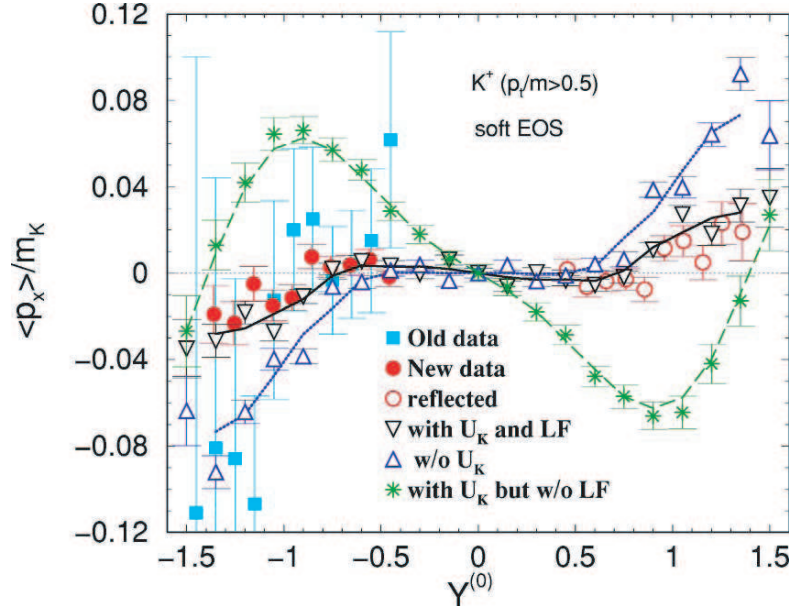


**Figure 3.2** The  $K^+$  transverse flow as a function of rapidity in 1.93 A GeV Ni + Ni reactions (Zheng, Fuchs, Amand Faessler, Shekhter, Srisawad, Kobdaj and Yan, 2004).

(Hermann and FOPI Collaboration, 1999) and their reflections at midrapidity, respectively. The theoretical results are given by the BRP with a soft EOS. The open down triangles stand for the calculated results with  $U_K$  and the Lorentz-force LF contribution, the open up triangles for the results without  $U_K$ , and the stars for the results with  $U_K$  but without LF. One sees that around midrapidity the two calculations with  $U_K$ &LF (static potential plus Lorentz force, open down triangles) and without  $U_K$  (open up triangles) almost coincide. The result without  $U_K$ , i.e., only including the kaon rescattering effect, predicts a slightly positive flow. The result with  $U_K$ &LF leads to a very small antiflow. Around midrapidity both calculations agree with the data within error bars. However, at spectator rapidities the two results with  $U_K$ &LF and without  $U_K$  differ substantially from each other. With respect to the old data set both calculations, i.e., with  $U_K$ &LF and without  $U_K$ , agree with experiment within error bars since both reproduce the

nearly vanishing side flow signal of  $K^+$ 's around midrapidity. This means that the old data can be reproduced without need for an in-medium kaon potential (David, Hartnack and Aichelin, 1999). However, the new data with much small error bars are only in agreement with those calculations which treat the kaon potential in the covariant kaon dynamics. This indicates that it is necessary to include the in-medium kaon potential in order to describe the new data for the  $K^+$  transverse flow.

From Fig. (3.2) it is seen that the strongly repulsive static potential tends to push the kaons dramatically away from the spectator matter, leading to a strong antiflow around midrapidity (stars). The effect of the LF contribution in the covariant kaon dynamics pulls the kaons back to the spectator matter, resulting in a finally reasonable pattern of the  $K^+$  transverse flow, which is in good agreement with the FOPI data. This feature of the LF contribution can also be seen in the calculations performed by the BRP with a hard EOS. This illustrates that the LF like contribution, originating from spatial components of the vector field, provides an important contribution to the in-medium kaon dynamics in heavy ion collisions. Kaons are produced in the early phase of the reaction where the relative velocity of projectile and target matter is large. Thus the kaons feel a nonvanishing baryon current in the spectator region, in particular in noncentral collisions. This contribution dramatically counterbalances the influence of the repulsive potential on the  $K^+$  transverse flow, leading to a reasonable fit to the FOPI data. This also shows that one can use the data of the  $K^+$  transverse flow to extract the information on the in-medium  $K^+$  potential.

The excitation function of the  $K^+$  cross sections in inclusive Au + Au and C + C reactions are shown in Fig. (3.3). Calculations are performed with  $b_{max} = 11$  fm for Au + Au and  $b_{max} = 5$  fm for C + C and are normalized to the experimental

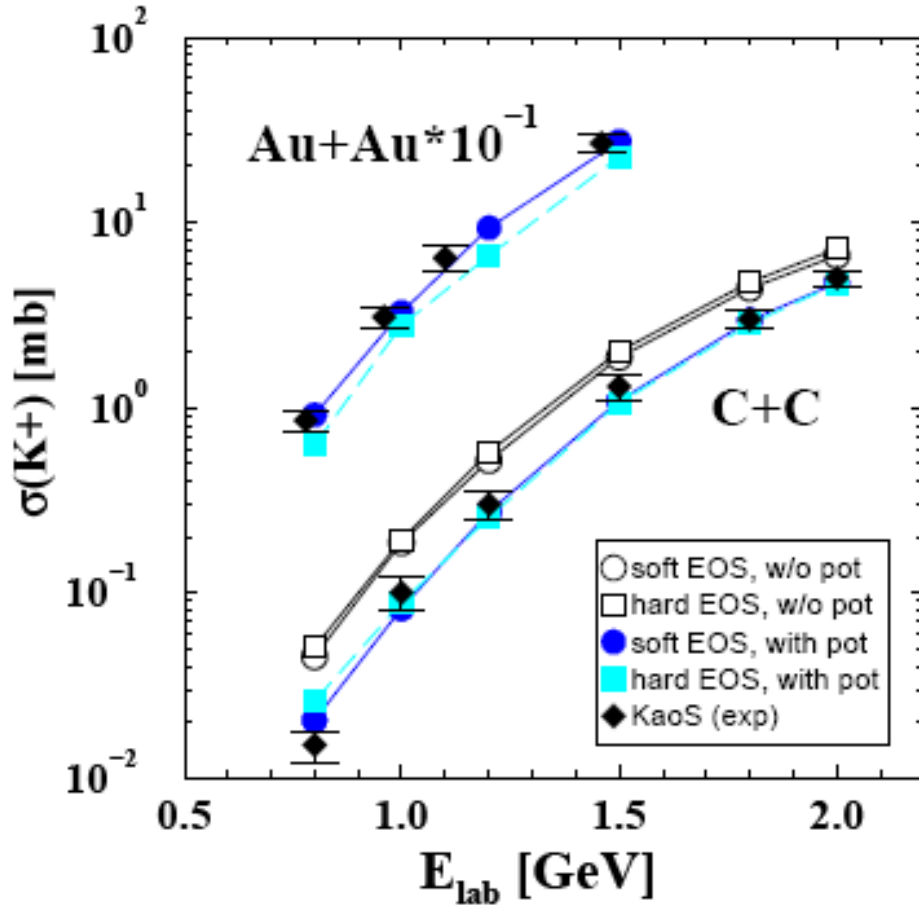


**Figure 3.3** The  $K^+$  excitation functions in Au + Au (scaled by  $10^{-1}$ ) and C + C reactions are compared to the KaoS data. Calculations include an in-medium kaon potential. For C + C results without in-medium kaon potential are also shown (Fuchs, Amand Faessler Zabrodin and Yu-Ming Zheng, 2001).

reaction cross sections. Calculations include an in-medium kaon potential. For C + C calculations without in-medium potential are also shown. It is seen that the results without kaon potential overestimate the data, while those with kaon potential are in good agreement with the data. This means that including of the in-medium  $K^+$  potential reduces the kaon yield, leading to a better fit to the data. This comparison supports again the existence of such a repulsive  $K^+$  potential.

The results for  $K^+$  kinetic energy spectra in Ni + Ni collisions at 0.8, 1.0 and 1.8 A GeV are shown in Figs. (3.4), (3.5) and (3.6), respectively. Calculations are performed using a soft nuclear EOS. The squares are the results with a in-medium  $K^+$  potential, the circles stand for the ones without the in-medium  $K^+$  potential. Diamonds are the Kaos data (Barth and Kaos Collaboration, 1997). One can see that the results without the in-medium  $K^+$  potential give the slope of the  $K^+$  kinetic energy spectra smaller than the experimental ones in the low c.m. kinetic energy region. The repulsive potential accelerates kaons and push they to the larger c.m. kinetic energy region during their propagation, leading an increase of the slope of the  $K^+$  kinetic energy spectra, which goes close the data ones. This feature is also seen clearly in Figs. (3.7), (3.8) and (3.9) when a hard nuclear EOS is used. This indicates again that the  $K^+$  meson is a good probe to extract the information on the in-medium  $K^+$  potential.

In Figs (3.10), (3.11) and (3.12) show the  $K^+$  production cross sections in Ni+Ni collisions at 0.8 , 1.0 and 1.8 A GeV with a soft/hard EOS and including the in-medium kaon potential, respectively. The error bars are given by the statistics. One sees from these figures that the agreement with data is good when a soft EOS is used. On other words, the KaoS data for the  $K^+$  production in Ni + Ni reactions strongly support the scenario with a soft EOS. It illustrates that the  $K^+$  meson is a suitable tool to probe the nuclear equation of state at high densities.

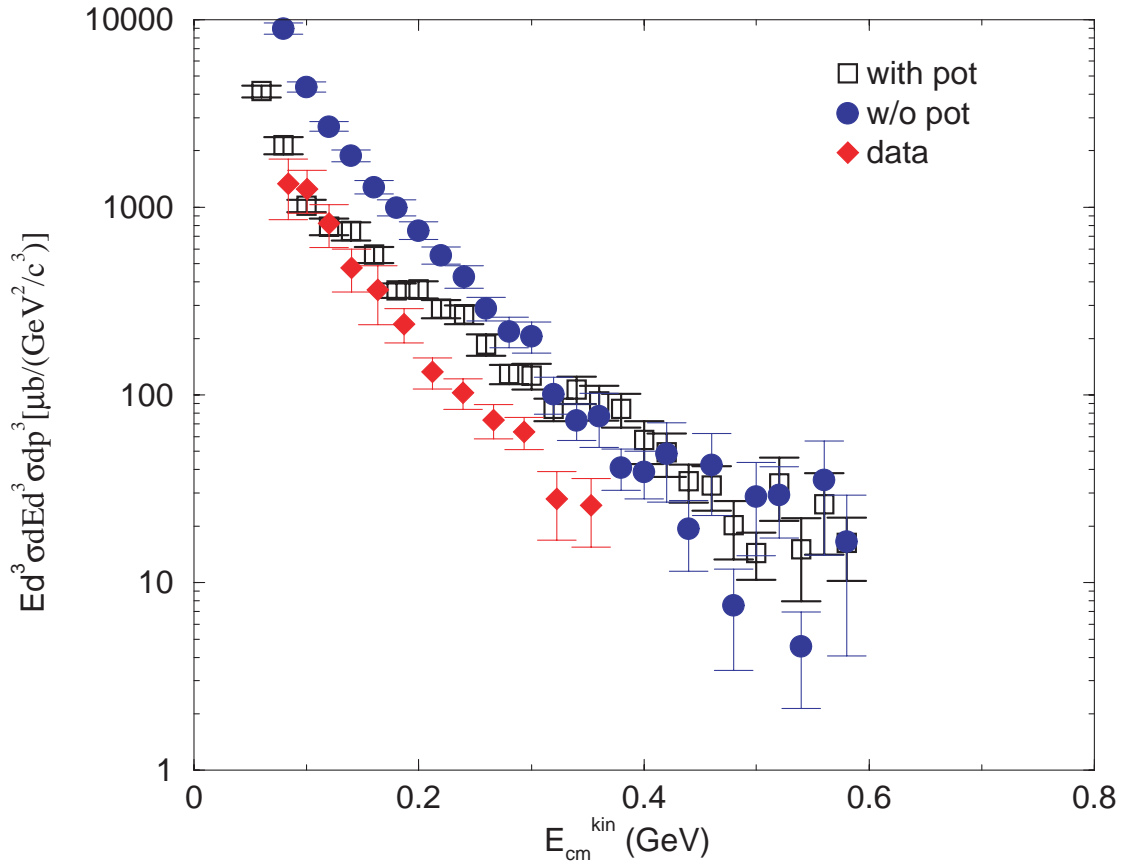


**Figure 3.4** Inclusive  $K^+$  production cross section for Ni + Ni collisions at 0.8 GeV/nucleon as a function of the c.m. kinetic energy. Calculations are performed using a soft nuclear EOS with and without kaon potential.



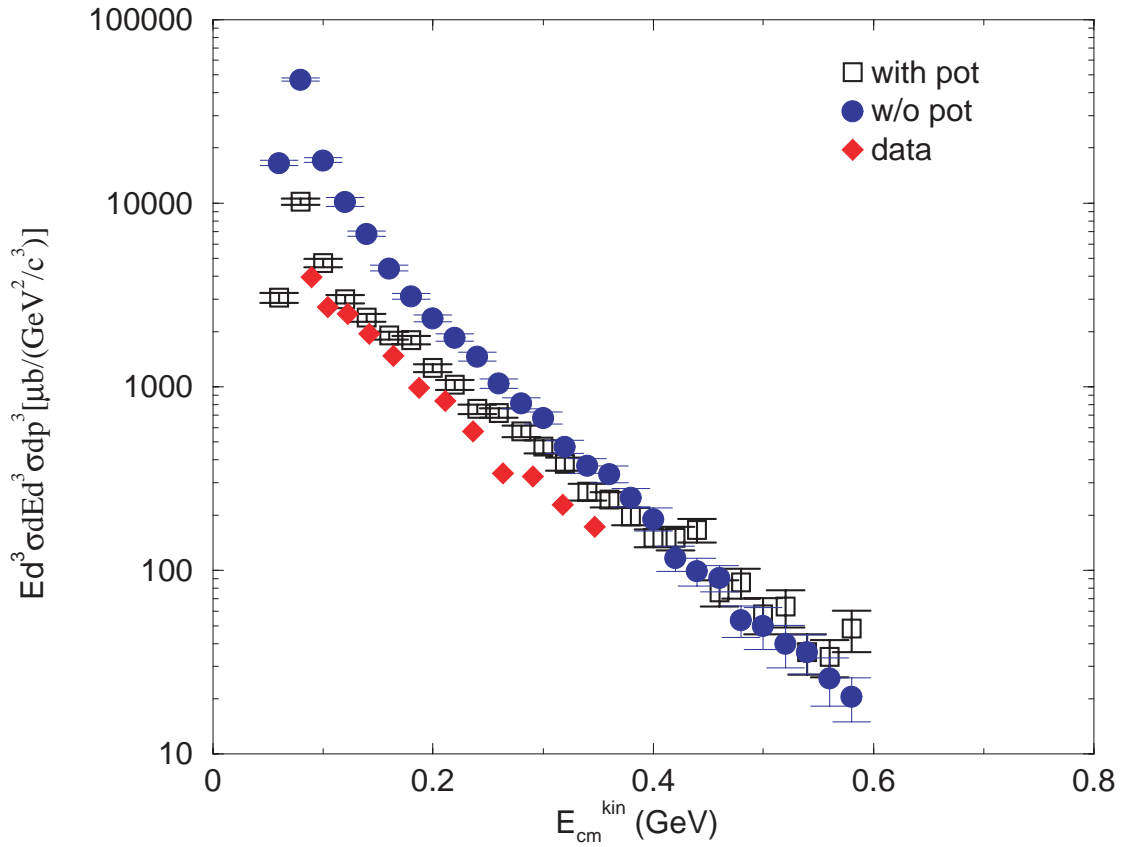


**Figure 3.5** Inclusive  $K^+$  production cross section for Ni + Ni collisions at 1 GeV/nucleon as a function of the c.m. kinetic energy. Calculations are performed using a soft nuclear EOS with and without kaon potential.

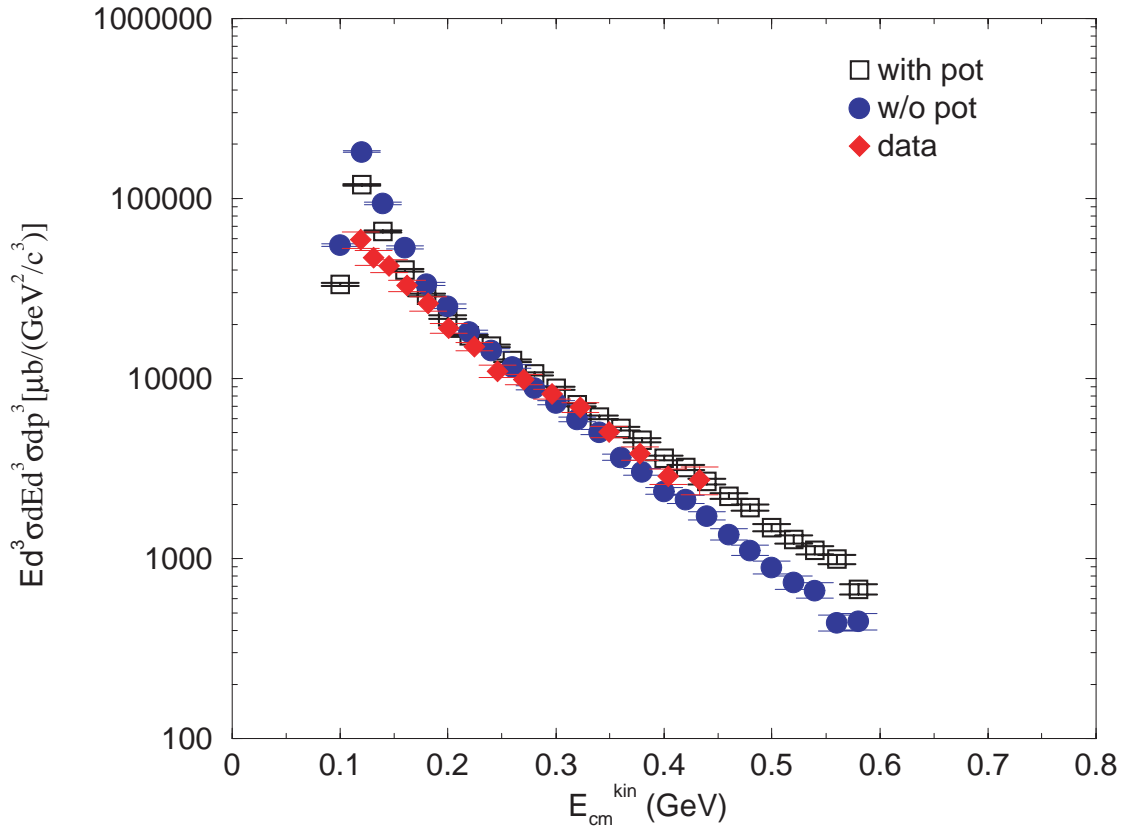


**Figure 3.6** Inclusive  $K^+$  production cross section for Ni + Ni collisions at 1.8 GeV/nucleon as a function of the c.m. kinetic energy. Calculations are performed using a soft nuclear EOS with and without kaon potential.

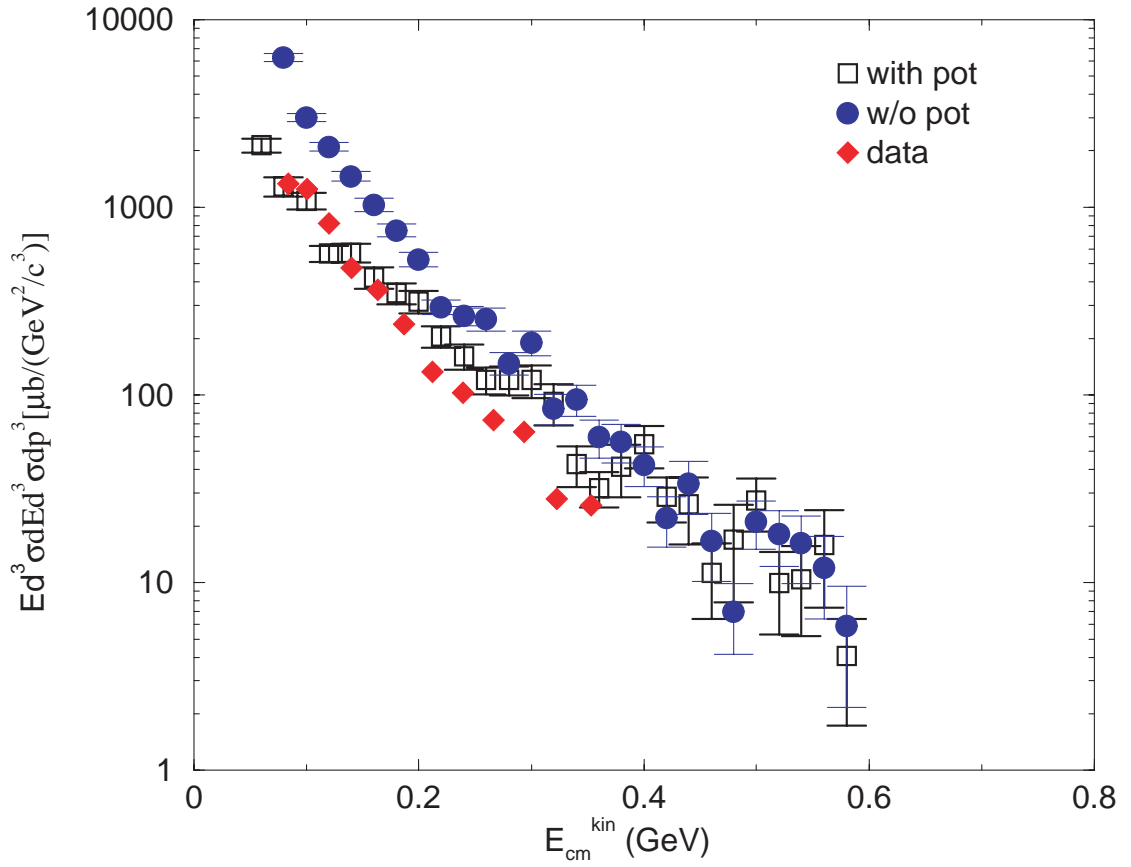


**Figure 3.7** Inclusive  $K^+$  production cross section for Ni + Ni collisions at 0.8 GeV/nucleon as a function of the c.m. kinetic energy. Calculations are performed using a hard nuclear EOS with and without kaon potential.

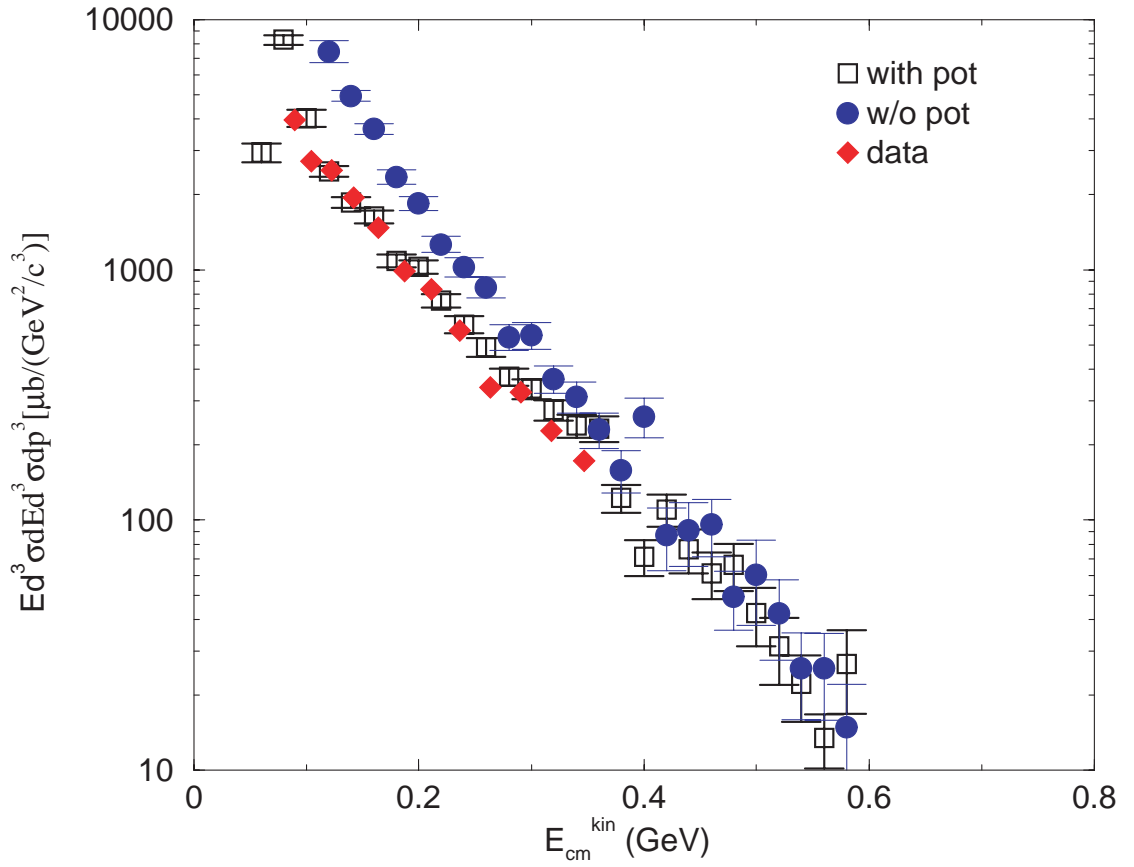


**Figure 3.8** Inclusive  $K^+$  production cross section for Ni + Ni collisions at 1 GeV/nucleon as a function of the c.m. kinetic energy. Calculations are performed using a hard nuclear EOS with and without kaon potential.

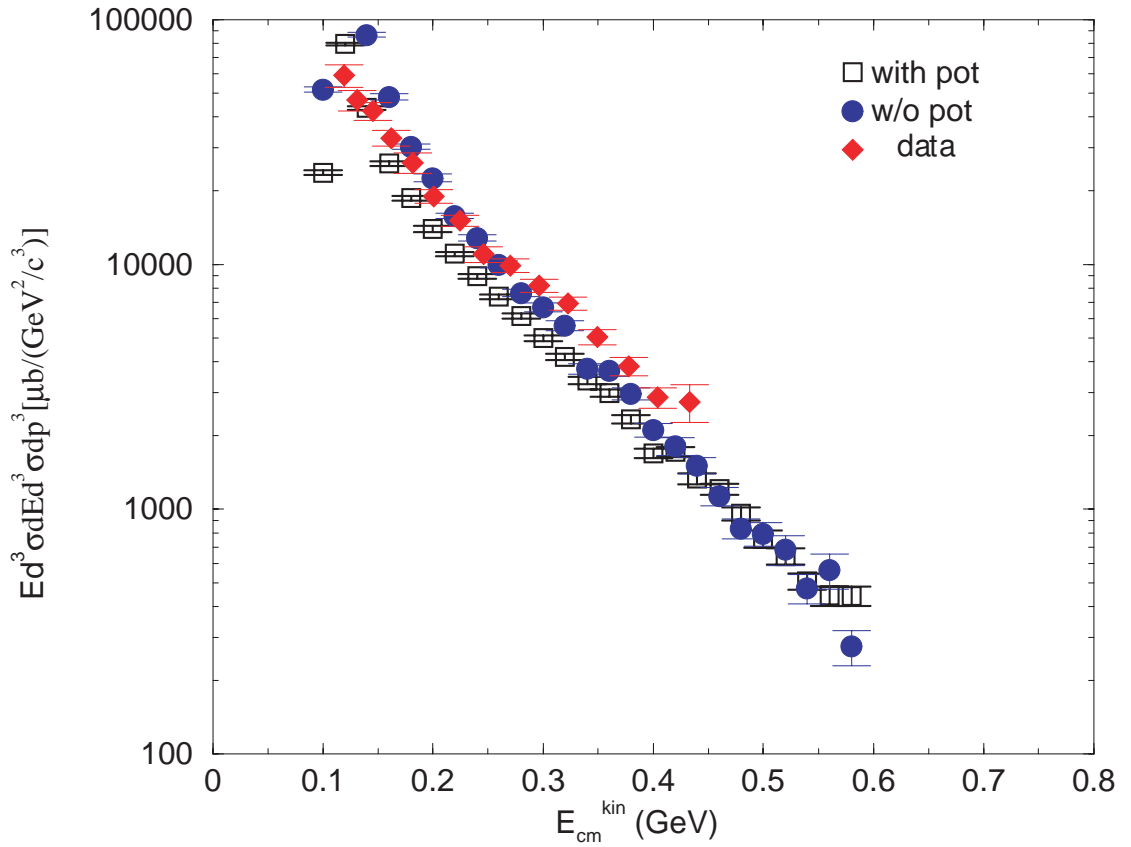


**Figure 3.9** Inclusive  $K^+$  production cross section for Ni + Ni collisions at 1.8 GeV/nucleon as a function of the c.m. kinetic energy. Calculations are performed using a hard nuclear EOS with and without kaon potential.

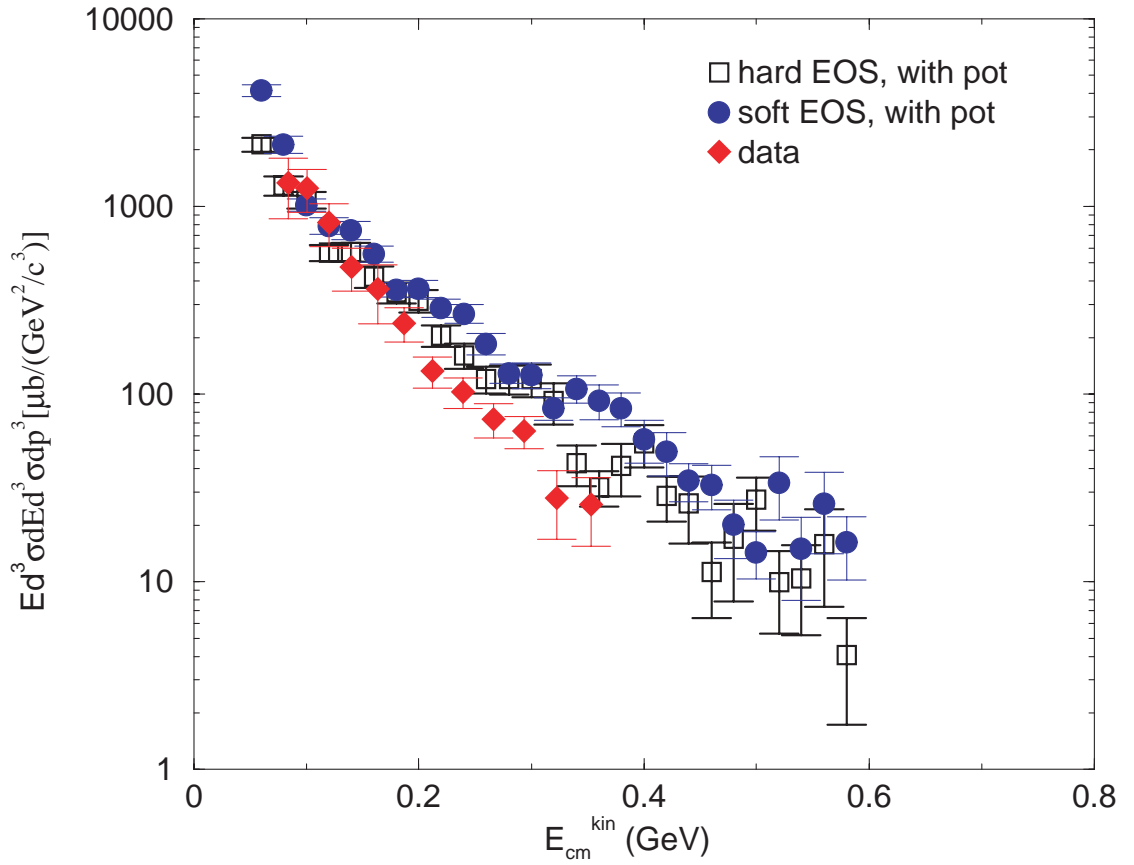


**Figure 3.10** Inclusive  $K^+$  production cross sections for Ni + Ni collisions at 0.8 GeV/nucleon as a function of the c.m. kinetic energy. Calculations are performed with an in-medium kaon potential and a hard/soft nuclear EOS.

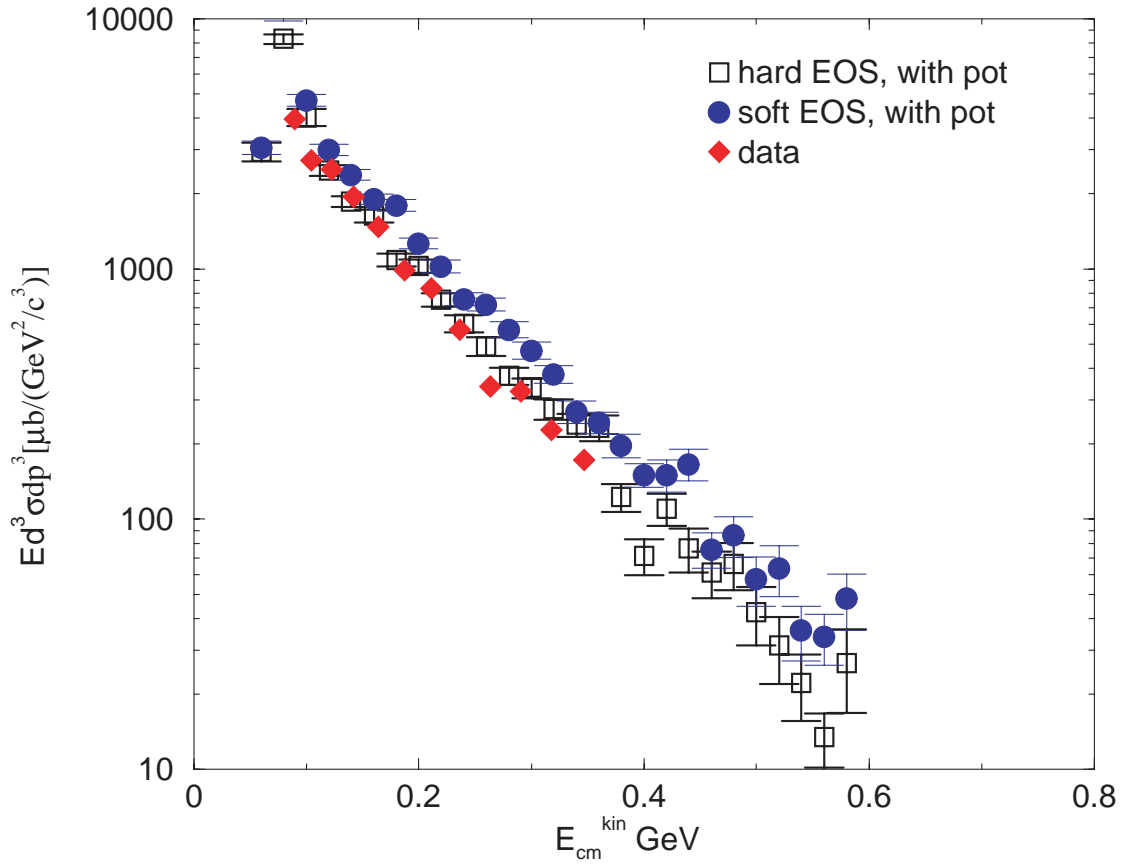


**Figure 3.11** Inclusive  $K^+$  production cross sections for Ni + Ni collisions at 1 GeV/nucleon as a function of the c.m. kinetic energy. Calculations are performed with an in-medium kaon potential and a hard/soft nuclear EOS.

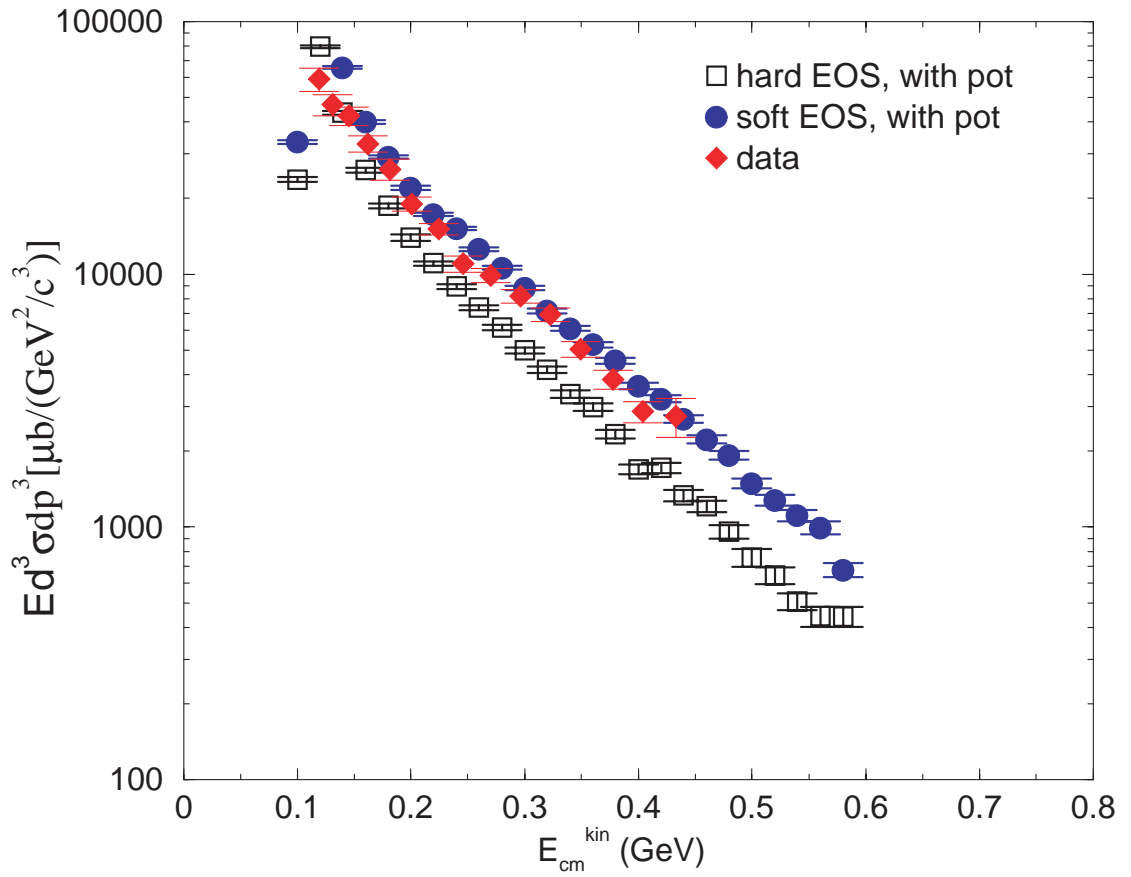


**Figure 3.12** Inclusive  $K^+$  production cross sections for Ni + Ni collisions at 1.8 GeV/nucleon as a function of the c.m. kinetic energy. Calculations are performed with an in-medium kaon potential and a hard/soft nuclear EOS.



# CHAPTER IV

## SIGMA MESON PRODUCTION IN HEAVY ION COLLISIONS

### 4.1 Sigma meson production in elementary reactions

One of the scheming properties of the Roper is its two-pion decay mode (Hernandez, Oset and Vicente Vacas, 2002). According to the Particle Data Group it has a 30 – 40 % branching ratio into  $N\pi\pi$  and a small fraction about 5 – 10 % going to  $N(\pi\pi)_{s\text{-wave}}^{I=0}$ . This scalar-isoscalar mode plays a very important role in all reactions involving two-pion production close to threshold. This isoscalar mode is a resonant state in the  $\pi\pi$  channel which can be associated with the scalar iso-scalar  $\sigma$  meson. The reason is that the contribution from the nucleon intermediate states cancels at threshold when the direct and crossed terms are taken into account. This has been shown explicitly in the pion-induced two-pion production (Oset and Vacas, 1985; Sossi, Fazel and Johnson, 1993; Bernard, Kaiser and Miesner, Ulf, 1995; Jensen and Miranda, 1997), the photon-induced two-pion production (Tejedor and Oset, 1994; Tejedor and Oset, 1996) and two-pion production from nucleon-nucleon collisions (Alvarez-Ruso, Oset, and Hernander, 1998; Alvarez-Ruso, 1999; Alvarez-Ruso, 2001).

The chiral symmetry is conserved if one assumes that the quark masses are zero. Since it is known that quarks have finite masses, this symmetry is spontaneously broken. This explains the existence of the pion and governs most of the low energy phenomena in hadron physics. An important consequence of the

spontaneous breakdown of a symmetry is the existence of a massless mode, the so called Goldstone-Boson. In our case, one obtains the pion as a Goldstone Boson and its chiral partner, the  $\sigma$  meson.

If chiral symmetry were a perfect symmetry of QCD, the pion would be massless. Since chiral symmetry is only approximate, we expect the pion to have a finite but small mass, compared to all other hadrons. This is indeed the case.

Low energy/temperature hadronic processes are dominated by pions and thus all observables can be expressed as an expansion in pion masses and momenta. This is the basic idea of chiral perturbation theory, which is very successful in describing threshold pion physics.

At high densities and/or temperatures one expects to ‘restore’ chiral symmetry. It means that the state at high density/temperature possesses the same symmetry as the Hamiltonian. As a consequence of this so called **“chiral restoration”** we expect the absence of any Goldstone modes and thus the pions. If it still present, it should become massive as well as its chiral partner the  $\sigma$  meson. To create a system of restored chiral symmetry in the laboratory is one of the major goals of the relativistic heavy ion experiments

The hadronic environment for relativistic heavy ion collisions is characterized by high temperatures ( $T \sim 170$  MeV) and low baryon densities ( $\rho \leq 0.2\rho_0$ ),  $\rho_0 = 0.16 \text{ fm}^{-3}$  is the saturation density of nuclear matter which is reached in the interior of heavy nuclei such as Pb. Such conditions are created in the collisions of heavy nuclei at the accelerator facilities at CERN/Geneva and at the “Relativistic Heavy Ion Collider” RHIC at Brookhaven/USA. In relativistic heavy ion collisions the environment can in first approximation be treated as a hot pion gas.

At intermediate energy heavy ion reactions, e.g. at the GSI/Darmstadt, the scenario is complementary: the temperatures are moderate ( $T \sim 50$  MeV) and

the baryon density is large ( $\rho \leq 3\rho_0$ ).

Detailed experimental and theoretical investigation of kaon production at intermediate energies shows clear indications for such a scenario. For vector-mesons  $\rho$  and  $\omega$  strong in-medium effects can also be expected.

For the  $\sigma$ -meson, which is not directly related to the phenomenon of chiral restoration, the experimental situation is not so clear. The  $\sigma$  is a broad resonance and the pole mass is even not precisely determined. Therefore the  $\sigma$  meson is very difficult to identify from the experimental side.  $\sigma$  meson production has not yet been measured in heavy ion reactions. Recently,  $\sigma$  meson production has been measured in pion and photon induced reactions on nuclei (Messchendorp, Janssen, Kotulla, Ahrens, et al., 2002). The existing data provide first indication for a mass shift of the  $\sigma$  in heavy nuclei (Bonutti, Camerini, Fragiaco, Grion, et al., 1996). There has an experimental program to measure this mass shift also in proton-nucleus collisions in Jülich. The aim of the present work is to make a prediction for such reactions and to investigate the possibility for the observation of such mass shifts.

## 4.2 $\pi\pi$ interaction

In the model of Oset and Coworkers (Vicente Vacas and Oset, 2004) one considers only the scalar isoscalar ( $\sigma$ ) channel and follows the simple method of the work (Oller and Oset, 1997) for  $\pi\pi$  interaction in vacuum (Chiang, Oset and Vacas, 1998; Oset and Vacas, 2000) and in the nuclear medium, which leads to modifications of the  $\sigma$  mass and width in a dense nuclear environment. In the following the approach of the work (Vicente Vacas and Oset, 2004) is shortly outlined.

### 4.2.1 $\pi\pi$ interaction in Vacuum

The  $\pi\pi$  interaction in nuclear matter has been calculated in the framework of a chiral unitary approach which generates the  $f_0$  and  $\sigma$  resonances, and reproduces well the meson-meson phase shifts in vacuum. The pions undergo multiple scattering which is accounted for by means of the Bethe-Salpeter (BS) equation, which guarantees unitarity, matching the low energy results to chiral perturbation theory ( $\chi$  PT) predictions. We consider two coupled channels,  $\pi\pi$  and  $K\bar{K}$ , and neglect the  $\eta\eta$  channel which is not relevant at the low energies we are interested in.

The BS equation is given by

$$T = V + VGT \quad (4.1)$$

Eq. (4.1) is a matrix integral equation, which involves the two meson one loop divergent integral. The diagram represented by this equation is depicted in Fig. (4.1), where V and T appear off shell. V is the bare  $\pi\pi$  interaction, taken from chiral perturbation theory, T is the T-matrix which contains the full sum of ladder diagrams. G is the two-pion propagator. However, for this channel both functions can be factorized on-shell out of the integral. The remaining off-shell part can be absorbed by a renormalization of the coupling constants (Oller and Oset, 1997; Nieves and Arriola, 1999). The VGT originally inside the loop integral becomes the product of V, G and T with V and T the on-shell amplitudes independent of the integration variables. Thus, the BS equation becomes purely algebraic. the  $2\pi$  propagator G is given by the expression

$$G_{ii}(P) = i \int \frac{d^4q}{(2\pi)^4} \frac{1}{q^2 - m_{1i}^2 + i\epsilon} \frac{1}{(P - q)^2 - m_{2i}^2 + i\epsilon}, \quad (4.2)$$

where P is the momentum of the meson-meson system. This integral is regularized

with a cut-off  $\Lambda=1.03$  GeV adjusted to fit to the  $\pi - \pi$  phase shifts. The potential  $V$  appearing in the BS equation is taken from the lowest order chiral Lagrangian,

$$L_2 = \frac{1}{12f_\pi^2} \langle (\partial_\mu \Phi \Phi - \Phi \partial_\mu \Phi)^2 + M\Phi^4 \rangle, \quad (4.3)$$

Where the the symbol  $\langle \rangle$  indicates the trace in flavour space,  $f_\pi = 93$  MeV is the pion decay constant, and  $\Phi$  and  $M$  are the pseudoscalar meson and mass SU(3) matrices, respectively. This model reproduces well phase shifts and inelasticities up to about 1.2 GeV. The  $\sigma$  and  $f_0(980)$  resonances appear as poles of the scattering amplitude. The coupling of channels is essential to produce the  $f_0(980)$  resonance, while the  $\sigma$  pole is little affected by the coupling of the pions to  $K\bar{K}$  (Oller and Oset, 1997).

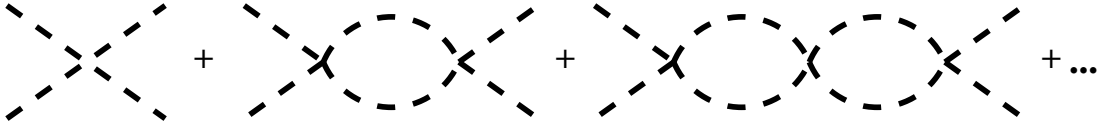


**Figure 4.1** diagrammatic representation of the BS equation for  $\pi\pi$  scattering in vacuum.

#### 4.2.2 $\pi\pi$ interaction in nuclear medium.

As we are mainly interested in the low energy region, which is not very sensitive to the kaon channels, we will only consider the nuclear medium effects on the pions. These are medium effects which appear in the intermediate state in the pion ladder. The main changes of the pion propagation in the nuclear medium come from the  $p$ -wave self energy, produced basically by the the coupling of pions to particle-hole ( $ph$ ) and Delta-hole ( $\Delta h$ ) excitations. For a pion of momentum  $q$  the self-energy  $\Pi(q)$ , which the pions require through this coupling to nucleon-hole

and Delta-hole state is given by

$$\Pi(q) = \frac{(\frac{D+F}{2f})^2 \vec{q}^2 U(q)}{1 - (\frac{D+F}{2f})^2 g U(q)}, \quad (4.4)$$

where the Landau-Migdal parameter  $g = 0.7$ ,  $U(q)$  is the Lindhard function,  $(D + F) = 1.257$ . The expressions for the Lindhard functions are taken from (Oset and Fernandez de Crdoba, 1990). Thus, the in-medium BS equation is given by the diagram of Fig. (4.2), where the solid line bubbles represent the  $ph$  and  $\Delta h$  excitations.

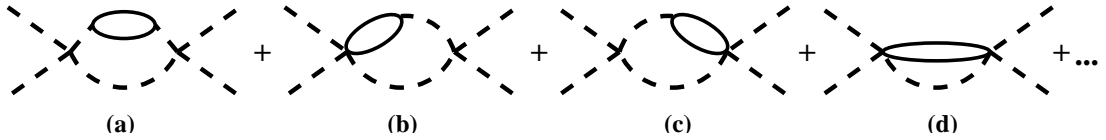


**Figure 4.2** Terms of the meson-meson scattering amplitude accounting for  $ph$  and  $\Delta h$  excitations

In fact, as it was show in (Chanfray and Davesne, 1999). the contact terms with the  $ph$  and  $\Delta h$  excitation of diagrams in Figs. (4.2) (b), (c) and (d) cancel the off-shell contribution of the meson-meson vertices in Fig. (4.2). Therefore, at the first order in baryon density, we are left with simple meson propagation corrections, which can be readily incorporated by changing the meson vacuum propagators to the in-medium ones.

At low densities, the  $\sigma$  meson can only decay into two pions:  $\sigma \rightarrow \pi + \pi$ . Therefore we have a threshold at  $E = 2m_\pi$ . The results for the  $\sigma$  pole position are shown in Fig. (4.3) for densities up to  $1.5\rho_0$ . The corresponding broadening of the in-medium widths are shown as well. Note, however, that the calculation is more reliable at low densities because some contributions of order  $\rho^2$  or higher are missing. We find that both mass and width decrease dramatically with increasing

of density, reaching a mass around 280 MeV and a similar width at  $1.5\rho_0$ . At large densities the  $2ph$  pieces of the pion self energy become relevant decreasing further both mass and width. The results in Fig. (4.3) can be cast in terms of an effective potential, which can be approximated by

$$V_\sigma = a\frac{\rho}{\rho_0} + b\left(\frac{\rho}{\rho_0}\right)^2, \quad (4.5)$$

with  $a = -358 - i108$  MeV and  $b = 140 + i23.6$  MeV. The in-medium potential  $V_\sigma$  given by Eq. (4.5) is used in our calculations.

Since the  $\sigma$  meson is an unstable particle, the potential  $V_\sigma$  is imaginary. The real part of  $V_\sigma$  provides the mean field, which leads to the mass shift of the  $\sigma$  meson inside the medium. The imaginary part determines the decay width  $\Gamma(\rho)$ .

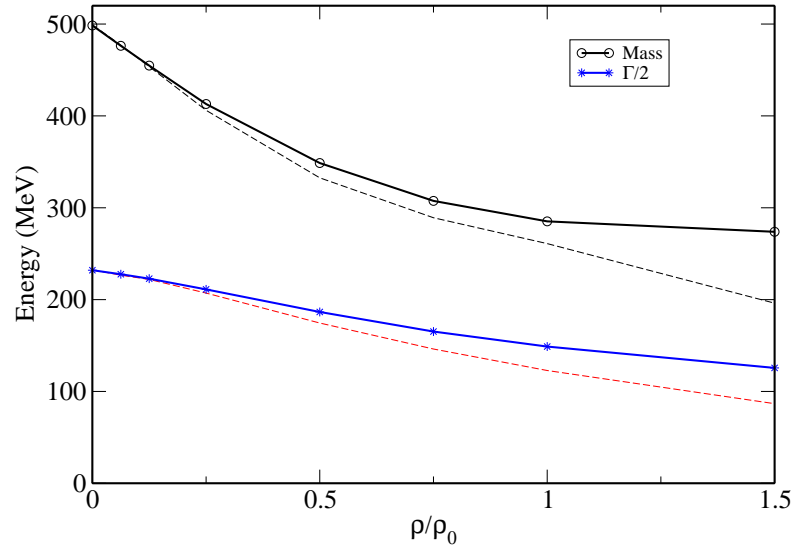


**Figure 4.3**  $\sigma$  mass and half width as the functions of the nuclear density. Dashed lines include also the  $2ph$  pion selfenergy pieces.

### 4.3 Sigma meson production in the QMD model

In the QMD model the sigma meson is produced via the decay of nucleon resonances  $N^*$

$$N^* \rightarrow N\pi\pi \quad (4.6)$$

with corresponding branching ratio. The  $N^*$ 's can be created via  $NB_1 \rightarrow B_2N^*$ , where  $B_i$  stands  $N$  or  $\Delta$ , and  $\pi N \rightarrow N^*$ . we take nucleons and the resonances  $\Delta(1232)$ ,  $N^*(1440)$ ,  $N^*(1520)$ ,  $N^*(1650)$  and  $N^*(1680)$  into account. In the  $N^* \rightarrow N\pi\pi$  decay the pion pair can occur in an isospin singlet s-wave state  $(\pi\pi)_{s-wave}^{I=0}$  with corresponding branching ratio. This state has the same quantum numbers as the  $\sigma$ -meson and is therefore identified with the  $\sigma$ -meson. The  $\sigma$ -mass is randomly chosen according to the Breit-Wigner distribution

$$dW_\sigma(\mu) = \alpha \frac{\mu\Gamma_\sigma^2 d\mu}{(\mu - m_\sigma)^2 + \mu\Gamma_\sigma}, \quad (4.7)$$

where  $m_\sigma$  is the pole mass and  $\mu$  the running mass of the  $\sigma$ -meson,  $\Gamma_\sigma$  is the  $\sigma$ -width. The normalization constant  $\alpha$  is determined by the available phase space, i.e. the mass of the decaying  $N^*$  resonance:

$$\frac{1}{\alpha} = \int_{2m_\pi}^{m_R - m_N} dW_\sigma(\mu), \quad (4.8)$$

where  $m_R$  is the resonance mass and  $m_N$  is the nucleon mass. Here one can see that the  $\sigma$ -meson can be assigned a value between the two-pion-threshold and the resonance mass minus nucleon mass. The resonance decays according to:

$$N(t) = N(0)e^{-\Delta t\Gamma/\gamma}. \quad (4.9)$$



The  $\sigma$  meson is a very broad scalar resonance, its life time is very small. It mainly decays into two pions in free space

$$\sigma \longrightarrow \pi\pi \quad (4.10)$$

#### 4.4 Results and discussions

The sigma mesons created during the collision, propagate inside the nucleus and decay after a short time inside the nucleus. The sigma meson can not be detected directly in an experimental setup, but there are indications towards its existence through the information collected from two pions that are measured in coincidence. During the QMD simulations every sigma and pion that is created is stored in some array and its evolution is followed through the end of the reaction. So we are able to get the whole number of  $\pi\pi$  that are a direct product of the sigma decay.

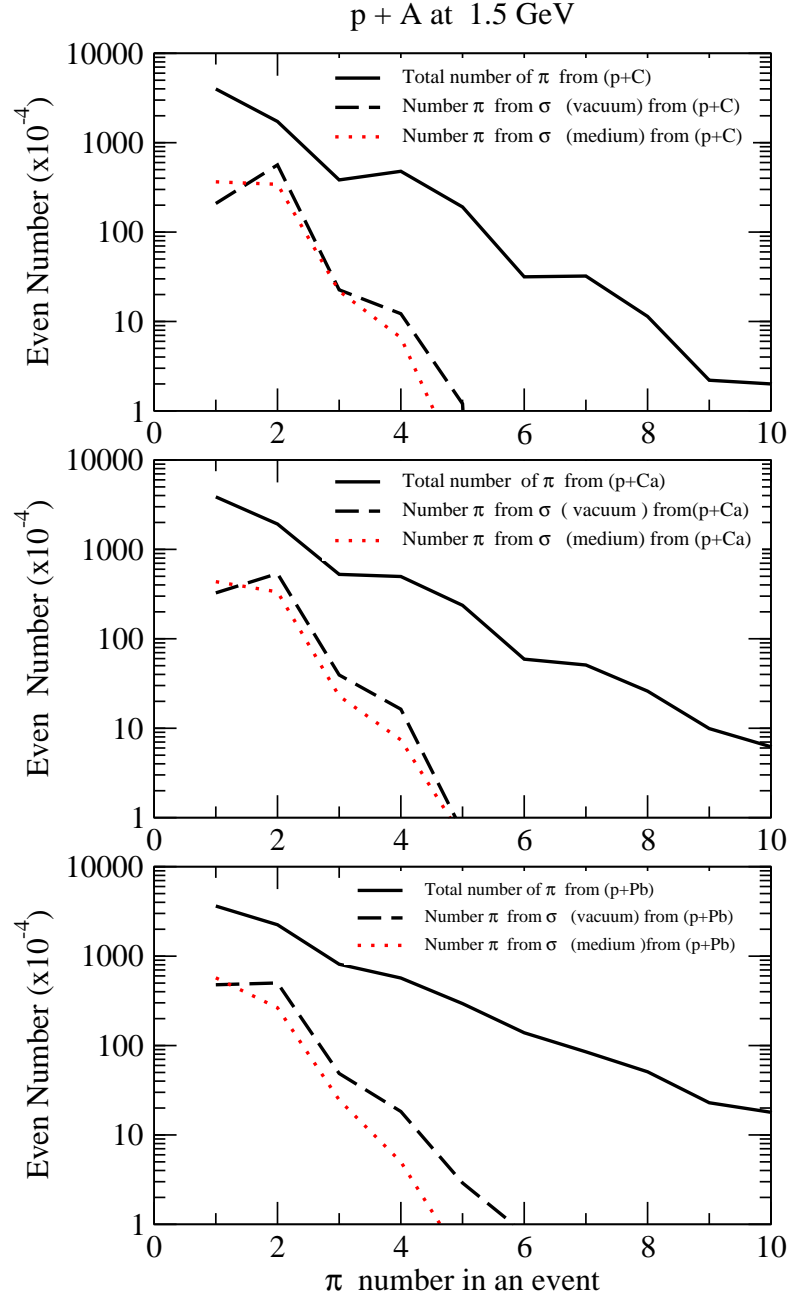


**Figure 4.4** The distribution of the  $\pi$  number produced in the p + A reactions with A being  $^{12}\text{C}$ ,  $^{40}\text{Ca}$  and  $^{208}\text{Pb}$  at the incident energy 1.5 GeV at the impact parameter  $b = 0$ .

In Fig. (4.4) shows the distribution of pion number produced in 1.50 GeV  $p + A$  ( $^{12}C$ ,  $^{40}Ca$  and  $^{208}Pb$ ) reactions at the impact parameter  $b = 0$ . The solid curve represents the total  $\pi$  number, the dashed and dot curves give the number of pions from  $\sigma$  meson decay without and with medium modifications, respectively. It is seen from this figure that the dashed and dot curves are about one order lower than the solid one in magnitude. This means that a large number of pions is produced, but only a few come from the  $\sigma$  meson decay. The results with medium modification show an even larger decrease in magnitude towards numbers of  $1\pi$ ,  $2\pi$  and  $3\pi$ , indicating the medium effect. One can also see a little the dependence of nucleus size on the produced pion numbers.

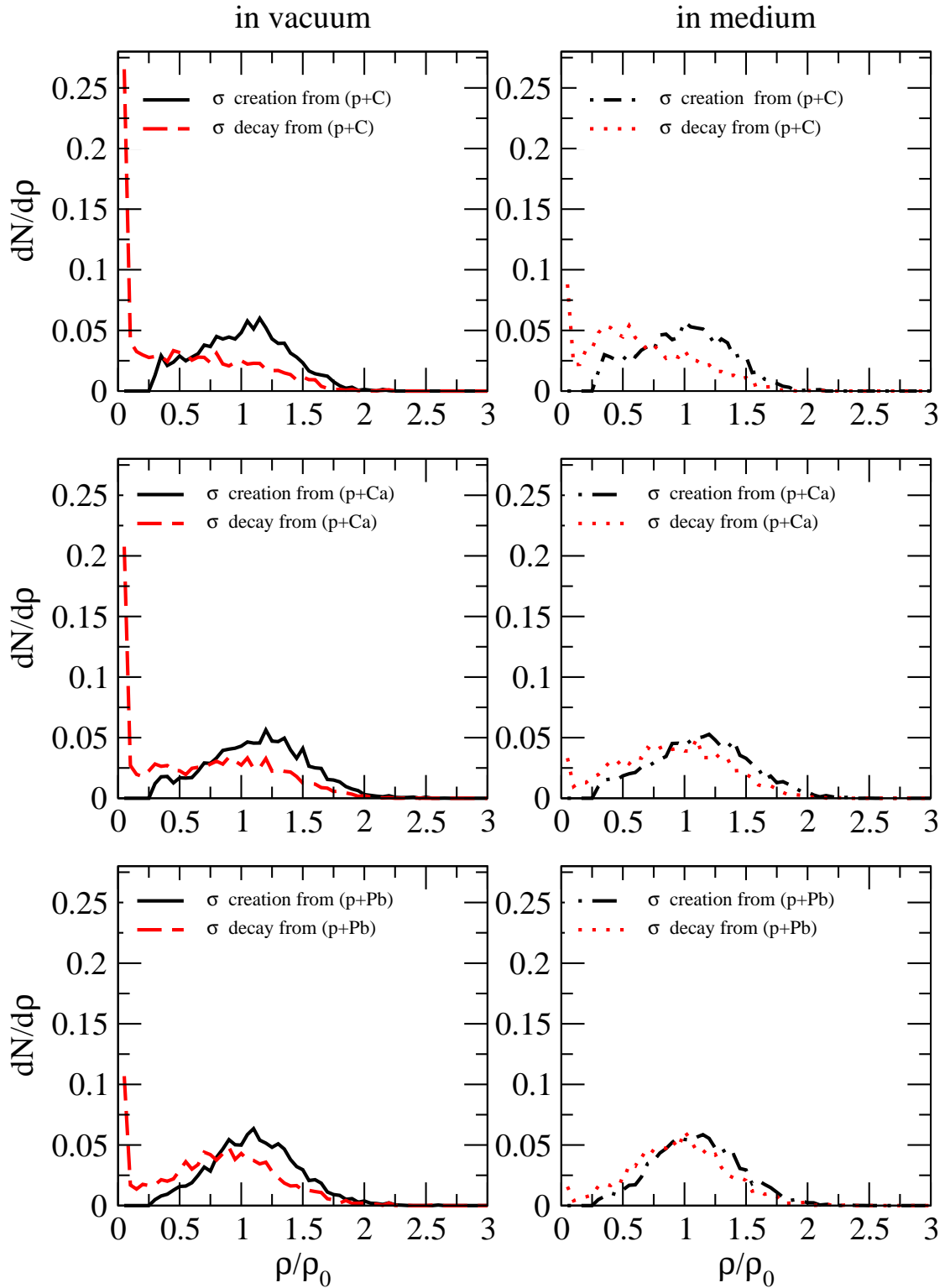


**Figure 4.5** The  $\sigma$  meson creation and decay as the function of the nuclear density ( $\rho$ ) in the  $p + A$  reactions with  $A$  being  $^{12}\text{C}$ ,  $^{40}\text{Ca}$  and  $^{208}\text{Pb}$  at the incident energy 1.5 GeV at the impact parameter  $b = 0$ .

In Fig. (4.5) shows the  $\sigma$  meson creation and decay as the function of the nuclear density without and with medium modifications. One sees from this figure that the features of the  $\sigma$  creation as the function of the nuclear density are weakly dependent on the nuclear medium. However, properties of the  $\sigma$  meson decay are significantly influenced by the nuclear medium. Without medium modifications most of  $\sigma$  mesons decay at the density close to zero and it is weakly dependent on the size of nucleus, while the decay mainly occurs at densities about  $\rho_0$  and depend obviously on the size of the nucleus when including the medium modifications. Because  $\sigma$  is a short lived resonance with life time  $\approx 10^{-24}$ sec and the in-medium  $\sigma$  potential is attractive and probably binds the  $\sigma$  inside the nucleus, the  $\sigma$  may decay at a higher density. It has to be noted that the incident proton leads to fluctuations of the densities. Thus compressing the nuclear matter to higher densities is locally possible. Therefore, the  $\sigma$  mesons may create and decay at densities above  $\rho_0$ , which is the maximal density inside the nucleus.

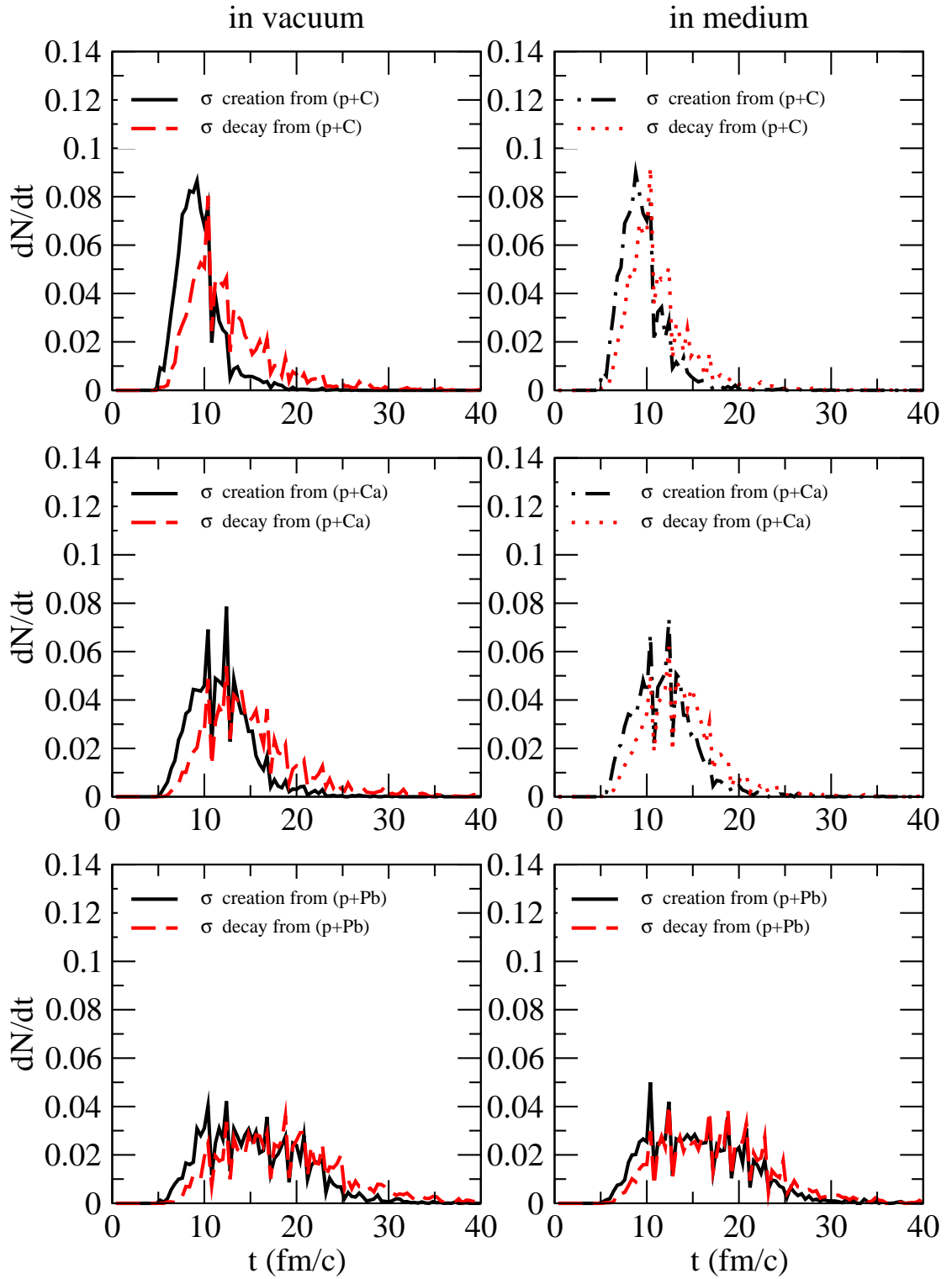


**Figure 4.6** The  $\sigma$  creation and decay probabilities as the function of time (fm/c) in the  $p + A$  reactions with  $A$  being  $^{12}\text{C}$ ,  $^{40}\text{Ca}$  and  $^{208}\text{Pb}$  at the incident energy 1.5 GeV at the impact parameter  $b = 0$ .

The probability distributions of the  $\sigma$  meson creation and decay in the  $p + A$  reactions with  $A$  being  $^{12}C$ ,  $^{40}Ca$  and  $^{208}Pb$  at the incident energy 1.5 GeV at the impact parameter  $b = 0$  are given in Fig. (4.6). It shows that the probability distributions of the  $\sigma$  meson creation and decay without and with medium modifications are almost peaked at time  $\approx 9$  fm/c and its width increases with increasing of the size of nucleus  $A$ . The creation and decay times are shifted by about 5 fm/c when the nucleus changes from light  $^{12}C$  to heavier  $^{208}Pb$ . As can be seen from this figure, most  $\sigma$  meson are created early and decay relatively later.

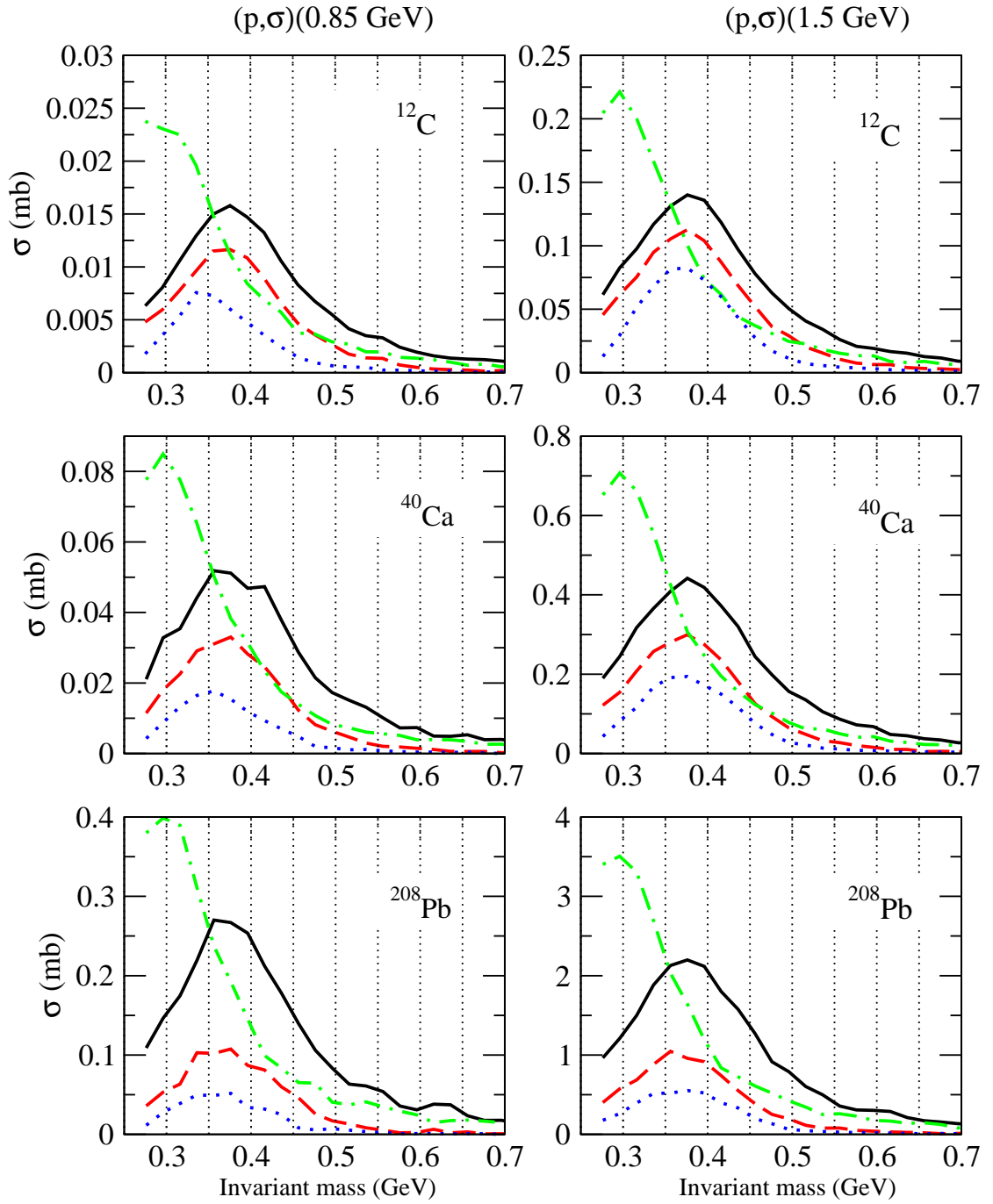


**Figure 4.7** The invariant-mass distribution of the sigma mesons produced in the  $p + A$  reactions with  $A$  being  $^{12}\text{C}$ ,  $^{40}\text{Ca}$  and  $^{208}\text{Pb}$  at the incident energies 0.85 GeV and 1.5 GeV. Solid lines: produced  $\sigma$  without medium modifications of the  $\sigma$  meson. Dashed lines: measured  $\sigma$  without medium modifications of the  $\sigma$  meson. Dot Dashed lines: produced  $\sigma$  with medium modifications of the  $\sigma$  meson. Dot lines: measured  $\sigma$  with medium modifications of the  $\sigma$  meson.



The solid curves and dot-dashed curves in the top of in Fig. (4.7) are the produced sigma mesons in  $^{12}C$  without and with medium modifications, respectively. We can see that the invariant mass distribution of sigma meson production shifts to the low invariant mass region due to the medium modifications. The density dependence of the  $\sigma$  mass shifts the curve to the low mass region when medium effect are taken into account. The dashed curves and dot curves in the figure are the measured sigma mesons without and with medium modifications, respectively. We can see also the same results for the shift of the measured sigma cross section to the low invariant mass region due to the medium modifications. In the second and third rows of Fig. (4.7) one sees the same results for  $^{40}Ca$  and  $^{208}Pb$ , respectively. The data points display a distinctive A dependence: the increase of A is followed by increase of the production cross sections. It is also shown in this figure that the cross section increase towards high energy is observed. The total  $\sigma$  production cross section increases with incident proton energy by about one order of magnitude when the proton energy increase from 0.85 to 1.5 GeV

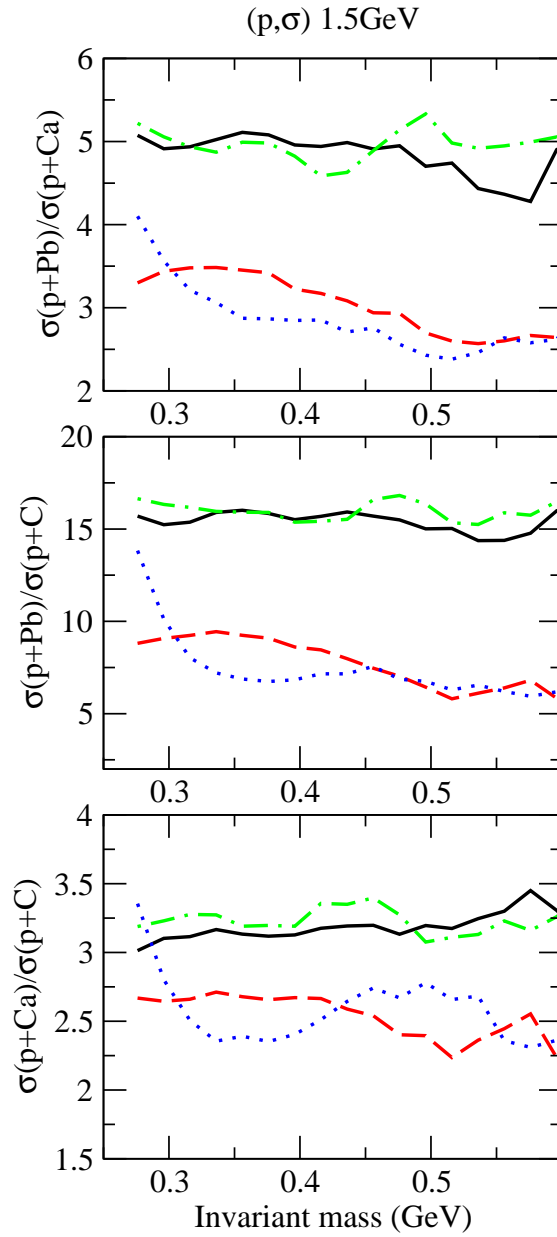


**Figure 4.8** Ratio of the sigma cross sections in various collisions. Solid lines: produced  $\sigma$  without medium modifications of the  $\sigma$  meson. Dashed lines: measured  $\sigma$  without medium modifications of the  $\sigma$  meson. Dot Dashed lines: produced  $\sigma$  with medium modifications of the  $\sigma$  meson. Dot lines: measured  $\sigma$  with medium modifications of the  $\sigma$  meson.

Shown in Fig. (4.8) are the ratio of the  $\sigma$  cross sections in various reactions. It is found from the larger values of the sigma production ratios  $\sigma(p + Pb)/\sigma(p + Ca)$  and  $\sigma(p + Pb)/\sigma(p + C)$  that the  $\sigma$  meson production in  $p + A$  collisions is strongly medium dependent. Without additional medium effects the ratio is almost constant as a function of the invariant  $\sigma$  mass when the shift of the  $\sigma$  mass is taken into account.

The ratios for the measured sigma show a significant enhancement at low invariant masses if the medium modification is considered. It indicates that the produced  $\sigma$  meson decaying in a denser medium experience a stronger mass shift towards lower masses since the medium is more dense in a heavier nucleus. It should be stressed that this mass shift is an experimentally accessible observable in the final state pion pairs which did not suffer reabsorption and rescattering by the surrounding nucleons. The ratio of measured sigma from various reactions opens the possibility to address experimentally the mass shift of the  $\sigma$  in a dense nucleus environment. In the other word, one can use the ratio of measured sigma from various reactions as a sensitive probe to extract the information on the in-medium  $\sigma$  potential.

# CHAPTER V

## SUMMARY

This thesis is a theoretical study of the kaon and sigma meson productions in heavy ion reactions at intermediate energies. The major purpose of the present study is to extract the information on the modifications of hadron properties in dense and hot nuclear matters and to explore the nuclear equation of state (EOS) at high densities. This issue is very important not only for nuclear and particle physics, but also for astrophysics. The medium dependence of the hadron properties is associated with the fundamental symmetries of the Quantum Chromodynamics (QCD), i.e. chiral symmetry and its breaking. The in-medium properties of strange hadrons belong to an issue which has significant implication on astrophysics concerning the evolution of neutron stars.

We describe the time evolution of the colliding nuclei within the framework of the Quantum Molecular Dynamics (QMD), in which the nucleon is described by a Gaussian wave packet with a constant width  $L$ . The time evolution of the N-body distribution is determined by the motion of the centroids of the Gaussians ( $\mathbf{r}_{i0}, \mathbf{p}_{i0}$ ), and the propagation of the Gaussians is described by the Poisson brackets. Two sets of parameters for the hard and soft equation of state (EOS) are used. One includes nucleons, deltas  $\Delta$ , the nucleon resonances  $N^*$  and  $\Delta$  resonances up to 2 GeV.

In this thesis we consider the bombarding energies of 0.8 - 2 GeV per nucleon for  $K^+$  meson production. This energy region is close to or even below the production threshold of the  $K^+$  meson in free nucleon-nucleon collisions. It

is thus expected that the  $K^+$  meson is a very ideal tool to probe the in-medium kaon potential and the nuclear EOS.

The variation of the hadron mass in a nuclear environment is related to a mean field experienced by the hadrons. The collective motion of the hadrons is very sensitive to the mean field. In the present study we have analyzed the  $K^+$  in-plane flow and the kinetic energy distributions of  $K^+$  production cross sections. For the kaon mesons inside the nuclear medium a quasi-particle picture including scalar and vector field is adopted. It is found that a Lorentz force from spatial component of the vector field provides an important contribution to the in-medium kaon dynamics and strongly counterbalances the influence of the vector potential on the  $K^+$  in-plane flow. The FOPI data can be reasonably described using the in-medium kaon potentials based on effective chiral models. The information on the in-medium  $K^+$  potential extracted from the kaon flow and the  $K^+$  production cross section as a function of their center-of-mass kinetic energy is consistent with the knowledge from other sources. On the other hand, it is confirmed that data of the  $K^+$  production cross sections are better described when a soft EOS is used.

It is known that the  $\sigma$  meson is responsible for the mid-range nucleon-nucleon attraction and plays an important role in the Quantum Hadrodynamics (QHD) and the nonlinear sigma model. However, the  $\sigma$  meson is a broad scalar resonance and mainly decays into two pions in free space. Thus the  $\sigma$  meson is commonly treated as an effective meson, that is, as a system of two pions coupled to the  $I = J = 0$  channel but not necessarily bound. Although the  $\sigma$  meson is not directly related to the phenomenon of chiral restoration, recently theoretical studies have shown that the  $\sigma$  mass  $m_\sigma$  and width  $\Gamma_\sigma$  decrease dramatically with increasing of the nuclear density  $\rho$ . This also means that the sigma meson may exist in a dense nuclear environment. There are also number of experimental efforts

to evidence the existence of the sigma meson by pion and photon induced reactions on nuclei. This causes great interesting to explore further the modification of sigma properties in nuclear medium. We investigate the sigma production in 1.5 GeV proton colliding on nuclei of  $^{12}C$ ,  $^{40}Ca$  and  $^{208}Pb$ . The simulation results indicate a distinctive  $A$  dependence of the sigma production, that is, the increase of  $A$  is followed by an increase of the production cross sections. It is found that the  $\sigma$  production in proton induced reactions is strongly medium-dependent, and the produced  $\sigma$  mesons decaying in a denser medium experience a stronger mass shift towards lower masses. This mass shift is an experimentally accessible observable in the final state pion pairs which did not suffer reabsorption by the surrounding nucleons. It is pointed out that the ratio of the measured sigma cross sections as a function of the sigma invariant-mass from various reactions can be used as a sensitive probe to extract the information on the in-medium  $\sigma$  potential.

## REFERENCES

## REFERENCES

- Aichelin, J. (1991), **Quantum molecular dynamics a dynamical microscopic n-body approach to investigate fragment formation and the nuclear equation of state in heavy ion collisions**, Physics Reports, Vol. 202, pp. 233-360.
- Aichelin, J. and Che Ming ko. (1985), **Subthreshold Kaon Production as a Probe of the Nuclear Equation of State**, Physical Review Letter, Vol. 55, pp. 2661-2663.
- Aichelin, J. and Stoecker, H. (1986), **Quantum molecular dynamics A novel approach to N-body correlations in heavy ion collisions**, Physics Letter B, Vol. 176, pp. 14-19.
- Alvarez-Ruso, L. (1999), **The role of the Roper resonance in  $np \rightarrow d(\pi\pi)^0$** , Physics Letter B, Vol. 452, pp. 207-213.
- Alvarez-Ruso, L. (2001), **Two-pion decay modes of the  $N^*(1440)$  in  $np \rightarrow d\pi\pi$** , Nuclear PhysicsA, Vol. 684, pp. 443-445.
- Alvarez-Ruso, L. Oset, E. and Hernander, E. (1998), **Theoretical study of the  $NN \rightarrow NN\pi\pi$  reaction**, Nuclear PhysicsA, Vol. 633, pp. 519-543.
- Barry, R. Holstein. (1995), **Chiral Perturbation Theory**, hep-ph/9510344.
- Barth, R. and Kaos Collaboration. (1997), **Subthreshold Production of Kaons and Antikaons in Nucleus-Nucleus Collisions at Equivalent Beam Energies**, Physical Review Letter, Vol. 78, pp. 4007-4010.



- Bass, S. A. (1998), **Microscopic models for ultrarelativistic heavy ion collisions**, Progress in Particle and Nuclear Physics, Vol. 41, pp. 255-369.
- Bernard, V., Kaiser, N. and Miener, Ulf-G. (1995), **The reaction  $\pi N \rightarrow \pi\pi N$  at threshold in chiral perturbation theory**, Nuclear PhysicsB, Vol. 457, pp. 147-172.
- Bertsch, G.F. and Kruse, H. (1984), **Boltzmann equation for heavy ion collisions**, Physical ReviewC, Vol. 29, pp. 673-675.
- Bethe H. A. and Brown G. E. (1995), **Observational constraints on the maximum neutron star mass**, Astrophysical Journal, Vol. 445, pp. 129-132.
- Boal, D. H. and Glosli, J. N. (1870), **Au as particle model for nuclear dynamics studies: Ground-state properties**, Physical ReviewC, Vol. 38, pp. 1870-1879.
- Bodmer, A. R. and Panos, C. N. (1977), **Classical microscopic calculations of high-energy collisions of heavy ions**, Physical ReviewC, Vol. 15, pp. 1342-1358.
- Boguta J. and Bodmer A. R. (1977), **Relativistic calculation of nuclear matter and the nuclear surface**, Nuclear PhysicsA, Vol. 292, pp. 413-428.
- Bonche, P., Koonin, S. and Negele, J.W. (1976), **One dimensional nuclear dynamics in the time-dependent Hartree-Fock approximation**, Physical ReviewC, Vol. 13, pp. 1226-1258.
- Bonutti F., Camerini, P., Fragiaco, E., Grion, N., Rui, et al. (1996), **A Dependence of the  $(\pi^+, \pi^+\pi^\pm)$  Reaction near the  $2m_\pi$  Threshold**, Physical Review Letter, Vol. 77, pp. 603-606.

- Bonutti F. et al. (1999),  **$\pi\pi$  pairs in nuclei and the  $\sigma$  meson**, Physical Review C, Vol. 60, pp. 018201.
- Bonutti F. et al. (2000), **The  $\pi\pi$  interaction in nuclear matter from a study of the  $\pi^+ A \rightarrow \pi^+ \pi^\pm A'$  reactions**, Nuclear PhysicsA, Vol. 677, pp. 213-240.
- Bratkovskay, E.L., Cassing, W. and Mosel, U. (1998), **Analysis of kaon production at SIS energies**, Nuclear PhysicsA, Vol. 622, pp. 593-604.
- Brown, G.E. and Awansom, E.S. (1994), **Kaon nucleon scattering amplitudes and  $Z^*$  enhancements from quark Born diagrams**, Physical Review C, Vol. 49, pp. 1166-1181.
- Brown G. E. and Rho M. (1991), **Scaling effective Lagrangians in a dense medium**, Physical Review Letter, Vol. 66, pp. 2720-2723.
- Brown, G.E. and Rho M. (1996), **From chiral mean field to Walecka mean field and kaon condensation**, Nuclear Physics, Vol. 596, pp. 503-514.
- Camerini P., Grion N. and Rui R. (1993), **Threshold behaviour of the  $\pi^+ \pi^-$  invariant mass in nuclei**, Nuclear PhysicsA, Vol. 552, pp. 451-468.
- Chanfray, G. and Davesne, D. (1999), **Pion interaction in nuclear matter and chiral symmetry restoration**, Nuclear PhysicsA, Vol. 646, pp. 125-138.
- Chiang, H. C., Oset, E. and Vicente Vacas, M. J. (1998), **Chiral nonperturbative approach to the isoscalar**, nucl-th/9712047.
- Christian Fuchs. (2006), **Kaon production in heavy ion reactions at inter-**

**mediate energies**, Progress in Particle and Nuclear Physics, Vol. 56, pp. 1-103.

Christian F., Amand Faessler., El-Basaouny S. and Zabrodin E. (2002), **The nuclear equation of state probed by  $K^+$  production in heavy ion collisions**, Journal of Physics G, Vol. 28, pp. 1615-1622.

Christian, F., Amand Faessler., Zabrodin, E. and Yu-Ming Zheng. (2001), **Probing the nuclear equation of state by  $K^+$  production in heavy ion collisions**, Physical Review Letter, Vol. 86, pp. 1974-1977.

Cugnon, J. (1980), **Monte carlo calculation of high-energy heavy-ion interactions**, Physical ReviewC, Vol. 22, pp. 1885-1896.

Cugnon, J., Kinet, D. and Vandermeulen, J. (1982), **Pion production in central high energy nuclear collisions**, Nuclear PhysicsA, Vol. 379, pp. 553-567.

Cusson, R.Y., Reinhard, P.G., Molitoris, J.J., Stoecker,H., Strayer, M.R. and Greiner, W. (1985), **Time-Dependent Dirac Equation with Relativistic Mean-Field dynamics Applied to Heavy-Ion scattering**, Physical Review Letter, Vol. 55, pp. 2786-2789.

Danielewicz, P. and Pratt, S. (1996), **Delays associated with elementary processes in nuclear reaction simulations**, Physical ReviewC, Vol. 53, pp. 249-266.

David C., Hartnack C. and Aichelin J. (1999), **On the flow of kaons produced in relativistic heavy-ion collisions**, Nuclear PhysicsA, Vol. 650, pp. 358-368.

- Davies, K.T.R. and Koonin, S.E. (1981), **Skyrme-Force time dependent Hartree-Fock calculations with axial symmetry**, Physical Review C, Vol. 23, pp. 2042-2061.
- Fuchs, C., Amand Faessler, Wang Z.S. and Gross-Boelting, T. (1999), **Chiral Kaon Dynamics in Heavy Ion Collisions**, Progress in Particle and Nuclear Physics, Vol. 42, pp. 197-206.
- Fuch, C., Kosov, D.S., Faessler Amand, Wang, Z.S. and Waindzoeh, T. (1998), **Consequence of covariant kaon dynamics in heavy ion collisions**, Physics Letter B, Vol. 434, pp. 245-250.
- Gasser J. and Leutwyler H. (1987), **Light quarks at low temperatures**, Physics Letter B, Vol. 184, pp. 83-88.
- Gasser J., Leutwyler H. and Sainio M. (1991), **Sigma-term update**, Physics Letter B, Vol. 253, pp. 252-259.
- Gell-Mann, Oakes and Renner. (1968), **Behavior of Current Divergences under  $SU_3 \times SU_3$** , Physical Review, Vol. 175, pp. 2195-2199.
- Gerber P. and Leutwyler H. (1989), **Hadrons below the chiral phase transition**, Nuclear Physics B, Vol. 321, pp. 387-429.
- Gomez Tejedor, J. A. and Oset, E. (1994), **A model for the  $\gamma p \rightarrow \pi^+ \pi^- p$  reaction**, Nuclear Physics A, Vol. 571, pp. 667-693.
- Gomez Tejedor, J. A. and Oset, E. (1996), **Double pion photoproduction on the nucleon: study of the isospin channels**, Nuclear Physics A, Vol. 600, pp. 413-435.

- Hatsuda, T. (2001), **Spectral change of hadrons and chiral symmetry**, hep-ph/v1.
- Hermann, H. and FOPI Collaboration. (1999), **Strangeness production and propagation in relativistic heavy ion collisions at SIS energies**, Progress in Particle and Nuclear Physics, Vol. 42, pp. 187-196.
- Hernandez, E., Oset, E. and Vicente Vacas, M. J. (2002), **The two pion decay of the Roper resonance**, Physical ReviewC, Vol. 66, pp. 65201-65207.
- Jaenicke, J., Aichelin, J., Ohtsuka, N., Lindenc, R. and Amand Faessler. (1992), **Intermediate-energy heavy-ion collisions with G-matrix potentials and cross sections**, Nuclear PhysicsA, Vol. 536, pp. 201-220.
- Jensen, T. S. and Miranda, A. F. (1997), **Low energy single pion production processes  $\pi N \rightarrow \pi\pi N$** , Physical ReviewC, Vol. 55, pp. 1039-1050.
- Jeukenne, J. P., Lejeune, A. and Mahaux, C. (1976), **Many-body theory of nuclear matter**, Physics Reports, Vol. 25, pp. 83-174.
- Kaplan, D.B. and Nelson, A.E. (1986), **Strange goes on in dense nucleonic matter**, Physics Letter B, Vol. 175, pp. 57-63.
- Ko, C.M. and Li, G.Q. (1996), **Medium effects in high energy heavy ion collisions**, Journal of Physics G, Vol. 22, pp. 1673-1726.
- Kogut J. B., Sinclair D. K. and Wang K. C. (1991), **Towards the continuum limit of the thermodynamics of lattice QCD with a realistic quark spectrum**, Physics Letter B, Vol. 263, pp. 101-106.
- Kruse, H., Jacak, B.V. and Stoecker, H. (1985), **Microscopic Theory of Pion**

**Production and Sideways Flow in heavy ion Collisions**, Physical Review Letter, Vol. 54, pp. 289-292.

Larionov, A. B., Effenberger, M., Leupold, S. and Mosel, U. (2002), **Resonance lifetime in Boltzmann-Uehling-Uhlenbeck theory: Observable consequences**, Physical ReviewC, Vol. 66, pp. 054604-054607.

Laue, F. and KaoS Collaboration. (1999), **Medium effects in kaon and antikaon production in nuclear collisions at subthreshold beam energies**, Physical Review Letter, Vol. 82, pp. 1640-1643.

Li, G.Q. and Ko, C.M. (1995), **Kaon flow in heavy ion collisions**, Nuclear PhysicsA, Vol. 594, pp. 460-482.

Li, G.Q., Ko, C.M. and Bao-An. (1995), **Kaon flow as a probe of the kaon potential in Nuclear medium**, Physical Review Letter, Vol. 74, pp. 235-238.

Li, G.Q., Ko, C.M. and Bao-An. (1997), **Kaon production in heavy ion collisions and maximum mass of neutron stars**, Physical Review Letter, Vol. 79, pp. 5214-5217.

Li, G.Q., Lee C.H. and Brown, G.E. (1997), **Kaons in dense matter, kaon production in heavy-ion collisions, and kaon condensation in neutron stars**, Nuclear PhysicsA, Vol. 625, pp. 372-434.

Machleidt R., Holinde K. and Elster Ch. (1987), **The bonn meson-exchange model for the nucleonnucleon interaction**, Physics Reports, Vol. 149, No. 1, pp. 1-89.

- Messchendorp J.G., et al. (2002), **In-Medium Modifications of the  $\pi\pi$  Interaction in Photon-Induced Reactions**, Physical Review Letter, Vol. 89, pp. 222302-222305.
- Molitoris, J., Hoffer, J. B., Kruse, H., and Stoecker, H. (1984), **Microscopic calculations of collective Flow probing the short-range nature of the nuclear force**, Physical Review Letter, Vol. 53, pp. 899-902.
- Nieves, J. and Ruiz Arriola, E. (1999), **Bethe-Salpeter approach for meson-meson scattering in Chiral perturbation theory**, nucl-th/980735.
- Oller, J. A. and Oset, E. (1997), **Chiral symmetry amplitudes in the s-wave isoscalar and isovector channels and the  $\sigma, f_0(98), a_0(980)$  scalar mesons**, hep-ph/9702314v1.
- Oset, E. and Fernandez de Crdoba, P. (1990), **Decay modes of sigma and lambda hypernuclei**, Physics Reports, Vol. 188, pp. 79-145.
- Oset, E. and Vicente Vacas, M. J. (1985), **A model for the  $\pi^-p \rightarrow \pi^+\pi^-n$  reaction**, Nuclear PhysicsA, Vol. 446, pp. 584L612.
- Oset, E. and Vicente Vacas, M. J. (2000), **Renormalization of the  $f_0(980)$  and  $a_0(980)$  scalar resonances in a nuclear medium**, Nucl-th/0004030.
- Petropoulos N. (2004), **Linear sigma model at finite temperature**, hep-ph/0402136.
- Ritman J.L. and FOPI Collaboration. (1995), **On the transverse momentum distribution of strange hadrons produced in relativistic heavy ion collisions**, Zeitschrift für Physik A: Hadrons and Nuclei, Vol. 352, pp. 355-361.

- Schaffner, J., Bondorf, J. and Mishustin I. N. (1997), **In-medium kaon production at the mean-field level**, Nuclear PhysicsA, Vol. 625, pp. 325-346.
- Schlagel, T.J., Kahana, S.H. and Pang, Y. (1992), **Forward protons and nuclear transparency in relativistic heavy-ion interactions**, Physical Review Letter, Vol. 69, pp. 3290-3293.
- Serot, B.D. and Walecka, J.D. (1986), **The Relativistic Nuclear Many Body Problem**, Advance Nuclear Physics, Vol. 16, pp. 1-327.
- Shekhter, K., Fuchs, C., Amand Faessler and Krivoruchenko, M. (2003), **Dilepton production in heavy-ion collisions at intermediate energies**, Physical ReviewC, Vol. 68, pp. 0149041-01490420.
- Sibirtsev, A. (1995), **Internal nuclear momentum and subthreshold kaon production**, Physics Letter B, Vol. 359, pp. 29-32.
- Sossi, V., Fazel, N. and Johnson, R. R. (1993),  **$^1H(\pi, 2\pi)$  cross sections with  $\pi\pi$  scattering derived from chiral lagrangians**, Physics Letter B, Vol. 298, pp. 287-291.
- Starostin A., et al. (2000), **Measurement of  $\pi^0\pi^0$  Production in the Nuclear Medium by  $\pi^-$  Interactions at 0.408 GeV/c**, Physical Review Letter, Vol. 85, pp. 5539-5542.
- Sturm, C. and KaoS Collaboration. (2001), **Evidence for a soft Nuclear Equation of state from Kaon Production in Heavy ion collisions**, Physical Review Letter, Vol. 86, pp. 39-42.
- Tang, H., Dasso, C. H., Esbensen, H., Broglia, R. A. and Winther, A. (1981), **Time evolution of Vlasov versus TDHF equations in the slab world**, Physics Letter B, Vol. 101, pp. 10-14.



- Teis, S. et al. (1997), **Pion-production in heavy-ion collisions at SIS energies**, Zeitschrift für Physik A: Hadrons and Nuclei, Vol. 356, pp. 421-435.
- Tsushima, K., Sibirtsev, A., Thomas, A.W. and Li, G.Q. (1999), **Resonance model study of kaon production in baryon-baryon reactions for heavy-ion collisions**, Physical ReviewC, Vol. 59, pp. 369-387.
- Tsushima, K., Huang, S.W. and Faessler, A. (1995), **Resonance model of pi Delta to YK for kaon production in heavy-ion collisions**, Journal of Physics G, Vol. 21, pp. 33.
- Uma Maheswari, V. S., Fuchs, C., Amand Faessler., Sehn, L., Kosov, D. S. and Wang, Z. (1998), **In-medium dependence and Coulomb effects of the pion production in heavy ion collisions**, Nuclear PhysicsA, Vol. 628, pp. 669-685.
- Vicente Vacas M. J. and Oset E. (2002), **Sigma meson mass and width at finite density**, nucl-th/0204055.
- Waas, T., Kaiser, N. and Weise, W. (1996), **Effective Kaon mass in dense nuclear and neutron matter**, Physics Letter B, Vol. 379, pp. 34-38.
- Walecka J. D. (1974), **A theory of highly condensed matter**, Annals of Physics, Vol. 83, pp. 491-529.
- Weise W. , (1993), **Nuclear aspects of chiral symmetry**, Nuclear PhysicsA, Vol. 553, pp. 59c-72c.
- Wolf M., et al. (2000), **Photoproduction of neutral pion pairs from the proton**, The European Physical Journal A, Vol. 9, pp. 5-8.

Yariv, Y. and Fraenkel, Z. (1981), **Intranuclear cascade calculation of high energy heavy ion collisions: Effect of interactions between cascade particles**, Physical Review C, Vol. 24, pp. 488-494.

Zheng, Y. M., Fuchs, C., Faessler Amand, Shekhter, K., Srisawad, P., Kobdaj, C, and Yan, Y. P. (2004), **Influence of the chiral mean field on the kaon in-plane flow in heavy ion collisions**, Communication in Theoretical Physics, Vol. 41, pp. 746-750.

Zheng Y. M., Fuchs C., Faessler Amand, Shekhter K., Yan Y. P., and Kobdaj Chinnorat. (2004), **Covariant Kaon dynamics and kaon flow in heavy ion collisions**, Physical ReviewC, Vol. 69, pp. 034907-034913.

# CURRICULUM VITAE

FIRST NAME: Pornrad

LAST NAME: Srisawad

GENDER: Female NATIONALITY: Thai DATE OF BIRTH: 26 October 1969

## EDUCATION BACKGROUND:

- Master of Engineering (Nuclear Technology), 1995, Chulalongkorn University, Bangkok, Thailand.
- Bachelor of Science in Physics, 1992, Naresuan University, Phitsanulok, Thailand.
- High School Diploma, 1987, Srilajarapipat School, Bangkok, Thailand.

## PUBLICATIONS:

- Y. M. Zheng, C. Fuchs, Amand Faessler, K. Shekhter, Pornrad Srisawad, Chinorat Kobdaj and Y. P. Yan. (2004). "Influence of the chiral mean field on the kaon in-plane flow in heavy ion collisions", *Commun. Theor. Phys.* 41: 746-750.
- Pornrad Srisawad, Yu-Ming Zheng, C. Fuchs, Amand Faessler, Yupeng Yan and Chinorat Kobdaj. (2006). Sigma meson production in heavy ion collision at intermediate energies. *Proceedings of the First National Symposium on Physics Graduate Research, CHEP07.*

## CONFERENCE:

- Participant, Summer School on Particle Physics on 13–24 June 2005, The Abdus Salam International Centre for Theoretical Physics, Trieste, Italy.

## SCHOLARSHIPS:

- Ministry of University Affairs of Thailand (MUA), 2001-2003.